Analytical and Finite Element Modelling for Static Analysis of Doubly Curved Spherical and Cylindrical Laminated Composite Shells

A Dissertation submitted

in partial fulfillment of the requirements for the degree of

Master of Engineering

in

MECHANICAL ENGINEERING

by

Lalit Kumar

Roll. No: 801584015

Under the supervision of

DR. NEERAJ GROVER

Assistant Professor, MED

MECHANICAL ENGINEERING DEPARTMENT, THAPAR UNIVERSITY

PATIALA

July, 2017

Certificate

This is certified that the work done in this thesis report title "Analytical and Finite Element Modelling for Static Analysis of Doubly Curved Spherical and Cylindrical Laminated Composite Shells " submitted in partial fulfillment of required for the award of Master of Engineering degree in CAD/CAM in the Mechanical Engineering department of Thapar University, Patiala, is an authentic record of work carried out by me under the guidance of Dr. Neeraj Grover, Mechanical Engineering department, Thapar University, Patiala. The matter embodied in this report has not been submitted in any part or full to any other university or institute for the award of any degree.

Lalit Kumar

Reg. No- 801584015

This is to certify that above declaration made by the student concerned is correct to the best of my knowledge and belief.

Date: 26/7/17.

Dr. Neeraj Grover

Assistant Professor, MED

Dedicated to

My father and mother

Acknowledgement

I would like to specially acknowledge and extend my heartfelt gratitude to all those who have helped me in completion of this seminar thesis report. With the biggest contribution, I would like to thanks Assistant Professor Dr. Neeraj Grover sir to full support and guidance.

Lastly, I would also like to thank my parents for this years of unyielding love and encourage. They have always wanted the best for me and I admire determination and sacrifice.

Abstract

In this present work, the static analysis of multilayered laminated composite spherical and cylindrical shells by using an inverse hyperbolic shear deformation theory (IHSDT) is presented. A non-polynomial shear strain shape functions (combination of inverse hyperbolic function) is used in the present theory which more accurately maps the shear strain in the transverse direction. The present IHSDT also produce results for plate as a special case. By implementing the purposed displacement field along with the strain-displacement relations, and constitutive relations in the virtual work principle, the governing equation are obtained in terms of five field variables. These equations are then solved using Navier-type, closed form solutions. The bending results are presented for cylindrical and spherical shells for simply supported boundary conditions. These shells are subjected to sinusoidal, distributed and point loads in transverse direction. The results are provided for thick to thin as well as shallow and deep shells. The present results are compared with the layer wise theory and with several other well-known higher order shear deformation theories (HSDTs). Further, the finite element numerical solutions are also presented for various other boundary conditions and compared with present IHSDT results and as well with various other HDST theories. The comparison of the present results reveals the applicability and validity of IHSDT both in analytical and finite element framework.

Keywords: Laminated composite shells, symmetric and anti-symmetric cross-ply, virtual work principle, Finite element method, shear deformation theory.

TABLE OF CONTENT

List of Figures

List of Tables

Nomenclature

ξ_1, ξ_2	Orthogonal Curvilinear Coordinate system
R_1, R_2	Radius of curvature along the mid-plane
ζ	Direction perpendicular to mid-plane
a_1, a_2	Vector perpendicular to axis along mid-plane
x, y	Cartesian Coordinate System
u, v	In-plane Displacements
$w, \bar{w}$	Dimensional and Non-Dimension Deflection
u_0, v_0, w_0	Mid-plane displacements
a, b, h	Length, Breadth and Thickness of the plate
θ_x, θ_y	Shear rotations
$\varepsilon_x, \varepsilon_y$	In-plane normal strains
γ_{xy}	In-plane shear strains
γ_{yz}, γ_{xz}	Transverse shear strain
Δ	Generalized displacement vector
$[Q]$	Transformation matrix
E	Elasticity Constant
ν	Poisson's Ratio
U	Total Strain energy
W	Work done
$\{F\}$	Force vector
$[R]$	Resultant stiffness matrix
q	Transverse load

Acronyms

CFS	Closed form solution
CLT	Classical Laminated Theory
ESL	Equivalent Single Layer
EDN	Equivalent Single Layer order N Polynomial
EDND	Equivalent Single Layer order N non- Polynomial
FSDT	First Order Shear Deformation Theory
HSDT	Higher Order Shear Deformation Theory
IHSDT	Inverse Hyperbolic Shear Deformation Theory
TSDT	Triangular Shear Deformation Theory
FEM	Finite Element Method
SSL	Sinusoidal Load
UDL	Uniformly Distributed Load

Chapter 1 Introduction

1.1. Basic concepts and Terminology

1.1.1. Composite Materials

The word composite means two or more material combined together on a macroscopic scale to form material which have far better engineering properties than conventional material. The composite material mostly made by combining *Fibre*, a reinforcement material and *Matrix*, a load carrying member of composite material. The material used mainly for fibre reinforcement are boron, silicon carbide, aluminium oxide, glass and carbon. *Matrix* a base material which provides the support to keep the fibres at desired location and orientation during loading condition and present in the continuous form in the composite material.it also protect the fibre material from the physical damage due to change of temperature and humidity. Material mainly used for matrix material are polymer, glass or ceramic.

The various properties have been improved over conventional structural materials are stiffness, strength, fatigue life, temperature dependent behaviour, thermal conductivity, corrosion resistance, thermal insulation and wear resistance.

1.2 Classification of Composite Material

The reinforcement of composite material are classified mainly in three category which is given below:

- Fibrous Composite
- Particulate Composite
- Laminated Composite

Fibrous composite, those composite which consist of fibres of one material in a matrix material of other.it also called lamina. Property of fibrous is depend upon the orientation of fibres in fibrous composite.it has very less thickness according to other two classification.

Particulate composite, those composite in which major constituents are particles of mica, silica, glass spheres, calcium carbonates etc.it don't contribute to the load carrying of the material but act as filler material for the matrix.

The main focus is on the third classification of composite, *laminated composite*. When two or more fibre- reinforced lamina or particulate composite stacked together and moulded in desired shape and

thickness. The most common form of laminated composite used for structural application is fibre-reinforced laminated composite.

The orientation of fibre-reinforced composite lamina during stacking allow wide range of physical and mechanical properties at the same volume fraction of fibre. The composites are designed according to structural requirement and loading conditions. Due to these unique feature it also called tailor made material. The considering case of cross-ply, this may reduce out our stiffness characteristics matrix element like *[A]*, *[B]*, and *[D]*. Orientation are plays a very important aspect to study because they may result in reduction or cancelation of the resultant forces and bending moments and twisting moments. The different orientation of lamina in laminated composite are discussed below:

Symmetric laminates, a laminate is considered to be symmetric if the material properties, angle and thickness of lamina are same below and above the mid-plane. Example for symmetric laminate is $\left[0^\circ/30^\circ/\overline{60^\circ}\right]_s$ as shown below.

0
30
60
30
0

For above example *[B]* = 0, this make the force matrix and momentum element are uncoupled in [B] matrix. If a laminate like this is subjected to force, it will lead to have zero mid-plane curvatures. Moreover, if it is subjected to moments only, it will give zero mid-plane strains. Due to symmetric laminate uncoupling between extension and bending will lot simpler our analysis for deflections and stresses.

Cross-Ply laminate, a laminate is considered to cross-ply laminate if unique 0° and 90° lamina is used to as stacking sequence for the composite or laminate. Example, cross-ply laminate $\left[0^\circ/90^\circ/90^\circ/0^\circ\right]$ as shown below.

0
90
90
0

For cross-ply laminate, $A_{16} = A_{26} = B_{16} = B_{26} = D_{16} = D_{26} = 0$, this shows that there is no coupling in-between the normal and shear forces , and also there is no coupling between the bending and twisting moments. By combine symmetric and cross-ply laminate by which coupling matrix *[B]* = 0 therefore force and momentum also uncoupled while analysis.

Angle-Ply laminates, a laminate is considered to be angle-ply laminate if lamina stack together in the oriented of $+\theta$ and $-\theta$ direction. An example of angle-ply laminate is $\left[-45^{\circ}/45^{\circ}/-45^{\circ}/45\right]$ as shown below.

-45
45
-45
45

For angle-ply laminate, if number of lamina are even, then $A_{16} = A_{26} = 0$. However if number of lamina are odd and it contain $+\theta$ and $-\theta$ alternate lamina, then not only it act as symmetric laminate as well as $A_{16}, A_{26}, D_{16}, D_{26}$ become small as the number of layers increase for the same laminate thickness. These type of laminate are good shear strength and stiffness properties.

Antisymmetric laminate, a laminate is considered to be antisymmetric if the laminate of same ply thickness and material are the same distance below and above the mid-plane with opposite orientation, an example of antisymmetric is shown below.

45
60
-60
-45

For antisymmetric laminate, the coupling terms $A_{16} = A_{26} = D_{16} = D_{26} = 0$.

Laminated composite further classification are given below:

- Laminated composite plates
- Laminated composite shells

Laminated Composite Plates, a composite is said to be a laminated composite plate if the different oriented fibre or material lamina stack together. Laminated composite have their

longitudinal dimensions one to two time the magnitude larger than their thickness. There are various theories present in the literature are given in last few decade for the structural analysis of laminated composite plates. The laminated composite plates analysed on the base of various span to thickness ratio (a/h).

Laminated Composite Shells, a composite is said to be a laminated composite shells if it has radius of curvature along both the x and y direction. The study of shells theories also permit the understanding of behaviour plates, curved beams, and flat beams structures as a special case. Shells are common structural elements in many engineering application include pressure vessels, submarine, ships hulls, wings , vertical tail of fuselages of airplanes, pipes and many more structures as a primary building material. Shells have more structural stiffness and load carrying capacity as compared to plates. Whereas the laminated composite shells are analyse on the bases of radius to thickness (R/a) ratio keeping span to thickness ratio as a constant. The shell are distinguish according to their laminated sequence.

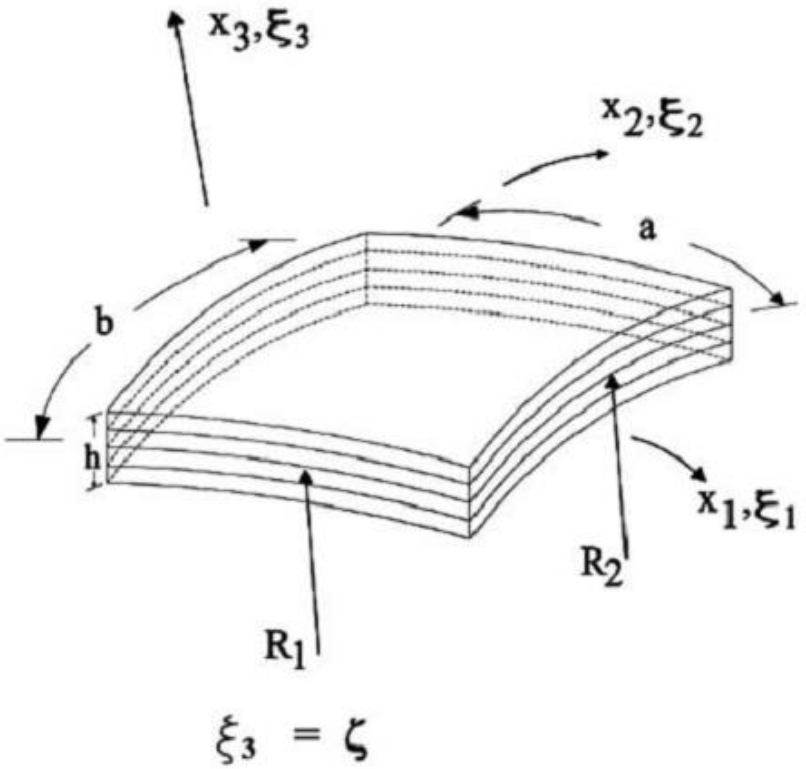

Figure 1.1: Geometrical representation of the laminated composite shell. Oktem et. al(2007)

1.3 Applications of composite materials

The application of composite materials for various primary structures due to their wide range of tailor made properties. Many industries trying to implement composite material for to replace conventional structural material. Various applications of composite material are illustrated below.

Aircraft: the military aircraft industry use the fibre polymer composites due to their light weight, more load carrying capacity. Due to significant reduction in weight of composites as a structural material, use of composite material for various commercial airlines aeroplane like Boeing 767 and A380. Composite also used as flooring of aeroplanes. In helicopters rotor blades are made up by use graphite/epoxy and glass/epoxy.

Space: Composite material used as doors of space shuttle because of better thermal properties and less in weight. Also used as cryogenic tanks. Advance antenna system and struts in satellite use graphite/epoxy. Composite material are used for light weight launch vehicles, mainly for nose cap, thermal protection system for space shuttles also developed using composite material.

Sports goods: Graphite/epoxy is used for golf club shafts to decrease the weight. Bicycles flames use graphite/epoxy composites to improve the stiffness of frame and reduce the overall weight. Tennis and racquetball rackets are also made of glass/epoxy due to light weight and stiffness. Ice hockey sticks as used composite materials due to high durability and stiffness.

Medical Devices: lightweight face masks for epileptic patients, artificial portable lungs are made of graphite-glass/epoxy. Composite materials also used for prosthetics body parts due to less cost and durability.

Marine: Fibre glass used for boats building material due to corrosion resistance property and kevlar-glass/epoxy to save weight, vibration damping characteristics. Housings are made now days of glass/epoxy and sustain pressures.

Automotive: the fibre glass body, leaf springs, bumpers, body panels and doors are made of composites.

Chapter 2 Literature Review

2.1 Introduction

The laminated composite spherical and cylindrical shells are significantly used as primary structural members in military, automobiles, sports, civil, aerospace and marine applications. These structures possess high specific strength, high specific stiffness, high resistance to corrosion, better impact strength, and capability for tailor-made designs. Moreover, the shells structures possess excellent compression and torsion resisting capabilities. The composite shells are multi-layered structures in which the several layers of orthotropic materials are perfectly bonded. These multi-layered structures are associated with shear deformation effects which must be adequately taken into consideration while modelling the geometry and structural kinematics of such structures.

2.2 Literature review on the laminated composite shells.

Theories were developed initially for thin shells on the base of the Kirchhoff-Love kinematic hypothesis. Love (1888), treated a thin plane plate is applied to the case of a thin shells, or plate of finite curvature. According to this theory the transverse shear strains is neglected in the transverse plane. Application of Kirchhoff-love theories give 30% or more errors in deflections, stresses as compared to various higher order theories.

Gulati et. al (1967) considered the case of anisotropic axisymmetric circular cylindrical shells is obtained employing an anisotropic shell theory given by naghdi which include the effect of transverse shear deformation. The field equations and boundary conditions of this theory involve only symmetric measures of strain and the symmetric parts of the stress resultant and stress couple tensors, and the constitutive equations meet all invariance requirements even after the introduction of first approximations. The displacement field of naghdi assumes the transverse normal displacement component to be independent of the thickness coordinate. The governing equations are solved by using Laplace transformation.

Whitny et. al (1974) purposed theory to analysis the anisotropic laminated cylindrical shells which include both transverse shear deformation and transverse normal strain. The validity if the theory was being assessed by comparing solutions obtained from the shell theory to

results obtained from exact theory of elasticity. Reasonably good agreement is observed and both shear deformation and transverse normal strain were shown in this paper was important for shells having a relatively small radius-to-thickness ratio. They compare results with exact elasticity theory.

Sanders Jr. (1959) used the principal of virtual work as the main derivative tool. The strain-displacement relation was predicted in this theory better then above mentioned theories. In the previous derivation on the basis of love hypothesis the number of unknown stress resultants and couples are reduced to 10 to 8 by making approximations in the expression for the resultants in terns if integrals of stress through the thickness of shell. But in this paper derivation reduction in number of stress unknowns for 10 to 8 was made by combining some of them in a way suggested by a certain expression of principle of virtual work which include the work done during a small rotation about the normal to the shell. The compatibility equations for the strain quantities involved in the theory lead directly to expressions for the stress resultants and couples in terms of a set of stress function. These expressions for the stress quantities satisfy the equations of equilibrium identically.

Reddy et. al (1984) in their work, the extended the sanders shells theory for double curved shells to a shear deformation theory of laminated shells presented first time. First time consider transverse shear strains and rotation about the normal to the shell mid-surface. Analytical solutions of the equations was presented for simply supported doubly curved cross-ply laminated shells under sinusoidal, uniformly distributed and point load at the centre. The analytical solution presented were become bench mark solution for future comparisons also know by name of FSDT.

Reddy et. al (1985) extension the work for higher-order shear deformation theory for elastic shells was developed for laminated orthotropic layered shells. It considered parabolic distribution of the transverse shear strain across the thickness of the shells and shear stress at top and bottom of shell structure is considered to be zero. The navier-type exact solution used for solving the set of governing equations. In this work they presented results for bending

and natural vibration under simply supported boundary condition for sinusoidal, uniformly distributed and point load.

Ren (1989) purposed an elastic solution for the analysis of a laminated circular cylindrical shell roof with simply-supported edge and the displacements and stresses of the solution are expressed in terms of infinite series, also provide a solution according to classical shell theory (CST). Computations for various ratios of mid-surface radius to thickness*(R/h)* for sinusoidal load had been examined with the elasticity solution results. Author used naiver-type exact solution method for solving sets of governing equations for deflection.

Chaudhuri et. al (1994) purposed a complete Fourier solution to the boundary–value problem of static response under transverse load of a general cross-ply thick doubly curved panel of rectangular platform. The sets of five governing partial differential equations were solved by fourier series approach. To generate the governing equation higher-order theory based upon shells approach with *SS2-type* of simply supported boundary condition prescribed for all four edges were used by the author. Author presented numerical accuracy of the solution by studying the convergence characteristics of deflections and moments of cross-ply spherical panels and also compared with the available first-order shear deformation theory and classical laminated theory based upon analytical solution.

Khara et. al (2003) presented a closed-form formulation of 2D higher-order shear deformation theories for the thermos-mechanical analysis of simply supported doubly curved cross-ply laminated shells. Author formulated the displacement model using polynomial form and converted 3-Dimensional elasticity problem into 2-Dimensional formulation form by using Taylor's series expansion. For solving the sets of governing equations author used naiver-type exact solution to get the values of deflection under sinusoidal load and provided results for various transverse normalized central deflection for symmetric and anti-symmetric cross-ply laminated shells.

Oktem et. al (2007) purposed an analytical solution using Levy-type method for the problem of deformation of a finite-dimensional general cross-ply thick double curved panel of rectangular plan-from using higher-order shear deformation theory (HSDT). A solution methodology, based on a boundary- discontinuous generalized double Fourier series approach used to solve a set of five highly coupled linear partial differential equation governing equation. The displacement field formulated by using non-polynomial shape function. Author used two different material properties with SS2-type simply supported boundary condition prescribed on two opposite edges and other two remained subjected to SS3-type constraint to formulate the problem for various normalized transverse central deflection with various radius to thickness *(R/a)* ratio and provide results for symmetric and anti-symmetric cross ply orthotropic laminated composite shells and cylinder under sinusoidal, uniformly distributed load. The numerical accuracy of solution were studied by the convergence of characteristics of deflections and moments of a moderated thick cross-ply spherical panel.

Mantari et. al (2012) purposed bending and free vibration analysis if multi-layered plates and shells by using higher order shear deformation theory (HSDT). Author defined displacement field using non-polynomial shear strain shape function (combination of exponential and trigonometric) taken from there pervious work.

Grover et al. (2014) purposed a new inverse hyperbolic shear deformation theory by introducing a new shear strain shape function which give non-linear distribution of transverse shear stress. The presented theory is implemented for static analysis of laminated composite and sandwich plates.

Masha et. al (2014) purposed a refined shell theories of isotropic and laminated shells. On the bases of higher expansion order for displacement field in the shell thickness direction a refined theory developed.

Tornabene et al. (2016) purposed results for laminated composite doubly-curved shells subjected to point and line load using polynomial based unified formulation.

Ferreira et al (2016) presented numerical results for functionally graded sandwich and laminated shells using layer-wise theory based on finite element modelling. Various micro mechanical models had been implement to predict accurate material property for laminated shells.

2.3 *Observation from literature review*

The literature review considering the modelling and analysis of laminated composite shells was performed and the following observations are made:

- The laminated composite shells are generally modelled using FSDT and PHSDT.
- The analysis of laminated shells with non-polynomial shear deformation theory is very limited.

2.4 Objective and Scope of the work

The objective of the present work is to examine the static response characteristics of laminated composite spherical and cylindrical shells in analytical and finite element framework

The following scope may be identified:

- Extension of IHSDT for doubly curved spherical and cylindrical shells originally developed for plates.
- Analytical solution for static analysis of laminated composite shells for symmetric and anti-symmetric cross-ply laminated composite spherical and cylindrical shell using IHSDT.
- Numerical solutions in the framework of Finite element analysis for static analysis of cross-ply laminated composite spherical and cylindrical shells.

3.1. Introduction

To study the static response of the laminated composite shells using the close-form analytical and Finite Element method is presented in this work. In context of axiomatic framework the displacement field is purposed with respect to higher order shear deformation theory and implemented in strain-displacement relation and constitutive relation to get the governing differential equation in terms of field variables for cross-ply laminated composite shells.

In order to examine the deformation characteristics of shell structure, a doubly curved laminated composite shell as shown in Fig. 3.1 is considered. The considered shell contain equal thickness orthotropic layers which are bounded perfectly. The shell geometry is shown in orthogonal curvilinear coordinates (ξ_1, ξ_2, ζ) where ξ_1 and ξ_2 are the lines of curvatures along $\zeta = 0$. The present formulation requires the implementation of displacement field, structural kinematic and constitutive relation in the principle of virtual work. A higher order shear deformation theory with inverse hyperbolic shear shape function is used with following assumptions as given below:

- Shear stress at top and bottom layer of shell are considered to be zero.
- Stress in each laminate is piece wise linear and Strain is linear along the transverse direction.
- Laminates are perfectly bounded.
- Small elastic deformation are assumed.

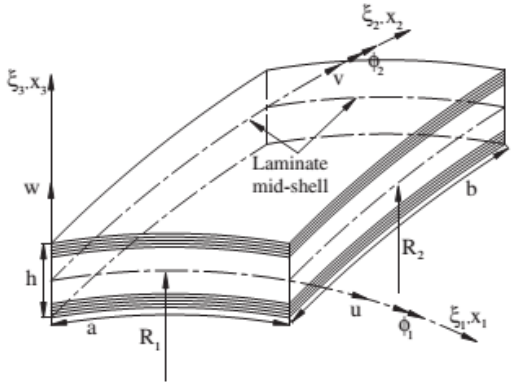

Figure 3.1: Laminated composite spherical shell geometry in orthogonal curvilinear coordinate system (Mantari et al., 2011)

3.2. Displacement field

A recently developed IHSDT by Grover et al. (2012) for laminated composite plates is extended for modelling of the laminated composite shells. In the framework of IHSDT, the displacement field is expressed axiomatically in terms of an inverse hyperbolic function of transverse coordinates. The tangential displacements (*u*, *v*) are functions of mid-plane displacements, mid plane rotations (θ_1, θ_2) and an inverse hyperbolic function. However, the transverses displacement (*w*) is assumed constant across the thickness of the shell and is equal to mid-plane transverse displacement. The IHSDT as applicable for laminated composite shells is given as follows:

$$\begin{aligned} u(\xi_1,\xi_2,\zeta) &= \left(1+\frac{\zeta}{R_1}\right)u_\circ - \zeta\frac{\partial w_\circ}{a_1\partial\xi_1} + \left(g(\zeta)+\Omega\zeta\right)\theta_1 \\ v(\xi_1,\xi_2,\zeta) &= \left(1+\frac{\zeta}{R_2}\right)u_\circ - \zeta\frac{\partial w_\circ}{a_2\partial\xi_2} + \left(g(\zeta)+\Omega\zeta\right)\theta_2 \\ w(\xi_1,\xi_2,\zeta) &= w_\circ \end{aligned} \tag{3.1}$$

Where $u_\circ, v_\circ, w_\circ$ are the mid-plane displacements while θ_1 and θ_2 are the shear rotations about ξ_1 and ξ_2, respectively. The terms *R1* and *R2* are the radii of curvatures along ξ_1 and ξ_2 directions respectively. Also, $f(\zeta) = g(\zeta) + \Omega\zeta$ in which $g(\zeta) = \sinh^{-1}(r\zeta/h)$ and $\Omega = -2r/\left(h\sqrt{r^2+4}\right)$. The parameter '*r*' is a shape parameter whose value is taken as 3.0. The tangent vectors to the line of curvatures ξ_1 and ξ_2 along the mid-plane are designated as a_1 and a_2.

3.3. Structural kinematics:

The shells under consideration are assumed to experience small deformation and small rotations. Under these assumptions, the structural kinematics of shells is expresses in the form of linear strain-displacement relations. The linear strain-displacement relations in the orthogonal curvilinear co-ordinate system are as follows:

$$\varepsilon_1 = \frac{1}{A_1}\left(\frac{\partial u}{\partial\xi_1} + \frac{1}{a_2}\frac{\partial a_1}{\partial\xi_2}v + \frac{a_1}{R_1}w\right)$$

$$\varepsilon_2 = \frac{1}{A_2}\left(\frac{\partial v}{\partial\xi_2} + \frac{1}{a_1}\frac{\partial a_2}{\partial\xi_1}u + \frac{a_2}{R_2}w\right)$$

$$\varepsilon_4 = \frac{1}{A_2}\frac{\partial w}{\partial \xi_2} + A_2\frac{\partial}{\partial \zeta}\left(\frac{v}{A_2}\right)$$
$$\varepsilon_5 = \frac{1}{A_1}\frac{\partial w}{\partial \xi_1} + A_1\frac{\partial}{\partial \zeta}\left(\frac{u}{A_1}\right) \qquad \text{(3.2a-3.2e)}$$
$$\varepsilon_6 = \frac{A_2}{A_1}\frac{\partial}{\partial \xi_1}\left(\frac{v}{A_2}\right) + \frac{A_1}{A_2}\frac{\partial}{\partial \xi_2}\left(\frac{u}{A_2}\right)$$

where $A_1 = (1+\zeta/R_1)a_1$, $A_2 = (1+\zeta/R_2)a_2$

Further, the strains are expresses in the form of primary field variables (mid-plane displacements and rotations) under the assumptions of small deformation and specifically for moderately deep and shallow shells. The strains in terms of primary field variables are expressed as:

$$\varepsilon_1 = \varepsilon_1^0 + z\left(\Omega\varepsilon_1^2 - \varepsilon_1^1\right) + g(z)\varepsilon_1^2$$
$$\varepsilon_2 = \varepsilon_2^0 + z\left(\Omega\varepsilon_2^2 - \varepsilon_2^1\right) + g(z)\varepsilon_2^2$$
$$\varepsilon_4 = g'(z)\varepsilon_4^0 + \Omega\varepsilon_4^1 \qquad \text{(3.3a-3.3e)}$$
$$\varepsilon_5 = g'(z)\varepsilon_5^0 + \Omega\varepsilon_5^1$$
$$\varepsilon_6 = \varepsilon_6^0 + z\varepsilon_6^1 + g(z)\varepsilon_6^2$$

where,

$$\varepsilon_1^0 = \frac{\partial u_\circ}{\partial x} + \frac{w_\circ}{R_1}, \quad \varepsilon_1^1 = \frac{\partial^2 w_\circ}{\partial x^2}, \quad \varepsilon_1^2 = \frac{\partial \theta_1}{\partial x}$$

$$\varepsilon_2^0 = \frac{\partial v_\circ}{\partial y} + \frac{w_\circ}{R_2}, \quad \varepsilon_2^1 = \frac{\partial^2 w_\circ}{\partial y^2}, \quad \varepsilon_2^2 = \frac{\partial \theta_2}{\partial y}$$

$$\varepsilon_4^0 = \theta_2, \quad \varepsilon_4^1 = \theta_2$$

$$\varepsilon_5^0 = \theta_1, \quad \varepsilon_5^1 = \theta_1$$

$$\varepsilon_6^0 = \frac{\partial v_\circ}{\partial x} + \frac{\partial u_\circ}{\partial y}, \varepsilon_6^1 = \Omega\frac{\partial \theta_2}{\partial x} + \Omega\frac{\partial \theta_1}{\partial y} - 2\frac{\partial^2 w_\circ}{\partial x \partial y}, \quad \varepsilon_6^2 = \frac{\partial \theta_2}{\partial x} + \frac{\partial \theta_1}{\partial y} \qquad \text{(3.4a-3.4e)}$$

$$g'(z) = \frac{rh}{\sqrt{r^2 z^2 + h^2}} \qquad \text{(3.5)}$$

The Cartesian coordinates $(a_1\partial\xi_1 = x, a_2\partial\xi_2 = y, \zeta = z)$ are related to the curvilinear coordinates as shown in Eq. (3.4a-3.4e).

3.4. Constitutive Relations

Each orthotropic layer of the considered shell possesses the linearly elastic stress-strain behaviour which is mathematically represented by the following constitutive relations:

$$\begin{Bmatrix} \sigma_{xx} \\ \sigma_{yy} \\ \tau_{xy} \\ \tau_{yz} \\ \tau_{xz} \end{Bmatrix}^{(k)} = \begin{bmatrix} \overline{Q_{11}} & \overline{Q_{12}} & \overline{Q_{16}} & 0 & 0 \\ \overline{Q_{12}} & \overline{Q_{22}} & \overline{Q26} & 0 & 0 \\ \overline{Q_{16}} & \overline{Q_{26}} & \overline{Q_{66}} & 0 & 0 \\ 0 & 0 & 0 & \overline{Q_{44}} & \overline{Q_{45}} \\ 0 & 0 & 0 & \overline{Q_{45}} & \overline{Q_{55}} \end{bmatrix}^{(k)} \begin{Bmatrix} \varepsilon_{xx} \\ \varepsilon_{yy} \\ \varepsilon_{xy} \\ \varepsilon_{yz} \\ \varepsilon_{xz} \end{Bmatrix}^{(k)} \tag{3.6}$$

or,

$$\{\sigma\}_{5\times1}^{(k)} = \left[\overline{Q_{ij}}\right]^{(k)} \{\varepsilon\}_{5\times1}^{(k)} \tag{3.7}$$

where $\left[\overline{Q_{ij}}\right]^{(k)}$ transformation reduced stiffness matrix depending upon the material properties(Young's modulus, Shear modulus and Possion's ratio) and fibre orientation (θ) of kth layer.

3.5. Analytical Modelling of cross-ply Laminated Composite shells

3.5.1. Derivation of Generalised Shell equations

The principle of virtual work as indicated in Eq. (3.8) is implemented to develop the governing differential equations of shells structures.

$$\int_0^T (\delta U - \delta V) dt = 0 \tag{3.8}$$

where δU is the virtual strain energy and δV is the virtual work done due to applied force. The expression for virtual strain energy and virtual work are given in Eq. (3.9a-3.9b):

$$\delta U = \int_{\Omega_\circ} \left\{ \int_{\frac{-h}{2}}^{\frac{h}{2}} \left(\sigma_{xx}\delta\varepsilon_{xx} + \sigma_{yy}\delta\varepsilon_{yy} + \tau_{xy}\delta\gamma_{xy} + \tau_{yz}\delta\gamma_{yz} + \tau_{xz}\delta\gamma_{xz} \right) dz \right\} dxdy$$

$$\delta V = \int_{\Omega_\circ} q\delta w_\circ dxdy \tag{3.9a-3.9b}$$

It should be noted that only transverse loads are assumed to be acting on the shell surface, therefore virtual work done due to applied forces in expressed in terms of virtual work done due to transverse loads (q). The expression for virtual strain energy and virtual work done are substituted in the principle of virtual work given in Eq. (3.9) and the virtual strains are expressed in terms of virtual field variables by implementing Eq. (3.3). The integration by parts and fundamental lemma of variational calculus are implemented to simplify the equations. In this process, the terms containing identical virtual displacements are algebraically solved and the coefficients of individual virtual displacements are equated to zero as evident from virtual work statement. The governing differential equations are thus, obtained in terms of stress and moments resultants per unit length and given in Eq. (3.10a-3.10e).

$$\delta u_\circ : \frac{\partial N_{xx}}{\partial x} + \frac{\partial N_{xy}}{\partial y} = 0$$

$$\delta v_\circ : \frac{\partial N_{yy}}{\partial y} + \frac{\partial N_{xy}}{\partial x} = 0$$

$$\delta w_\circ : \frac{N_{xx}}{R_1} + \frac{N_{yy}}{R_2} - \frac{\partial^2 M_{xx}}{\partial x^2} - \frac{\partial^2 M_{yy}}{\partial y^2} - 2\frac{\partial^2 M_{xy}}{\partial x \partial y} + q = 0 \qquad \text{(3.10a-3.10e)}$$

$$\delta\theta_1 : \Omega\frac{\partial M_{xx}}{\partial x} + \frac{\partial P_{xx}}{\partial x} + \Omega\frac{\partial M_{xy}}{\partial y} + \frac{\partial P_{xy}}{\partial y} - Q_2 - K_2 = 0$$

$$\delta\theta_2 : \Omega\frac{\partial M_{yy}}{\partial y} + \frac{\partial P_{yy}}{\partial y} + \Omega\frac{\partial M_{xy}}{\partial x} + \frac{\partial P_{xy}}{\partial x} - Q_1 - K_1 = 0$$

The stress and moment resultants appearing in governing differential equations are defined as mentioned in Eq. (3.11a-3.11b).

$$\begin{bmatrix} N_{xx} & M_{xx} & P_{xx} \\ N_{yy} & M_{yy} & P_{yy} \\ N_{xy} & M_{xy} & P_{xy} \end{bmatrix} = \int_{\frac{-h}{2}}^{\frac{h}{2}} \begin{Bmatrix} \sigma_{xx} \\ \sigma_{yy} \\ \tau_{xy} \end{Bmatrix} \begin{bmatrix} 1 & z & z^2 \end{bmatrix} dz$$

$$\begin{bmatrix} Q_1 & K_1 \\ Q_2 & K_2 \end{bmatrix} = \int_{\frac{-h}{2}}^{\frac{h}{2}} \begin{Bmatrix} \tau_{xx} \\ \tau_{yy} \end{Bmatrix} \begin{bmatrix} 1 & g'(z) \end{bmatrix} dz \qquad \text{(3.11a-3.11b)}$$

The governing differential equations are further expressed in terms of fundamental field variables by implementing the stiffness integrals indicated in Eq. (3.12a-3.12b).

$$\left[A_{ij} \quad B_{ij} \quad D_{ij} \quad E_{ij} \quad F_{ij} \quad H_{ij}\right] = \int_{\frac{-h}{2}}^{\frac{h}{2}} \left[\overline{Q_{ij}}\right]\left[1 \quad z \quad z^2 \quad g(z) \quad zg(z) \quad (g(z))^2\right] dz \tag{3.12a}$$

For i, j = 1, 2, 4, 5 and 6.

$$\left[K_{ij} \quad L_{ij}\right] = \int_{\frac{-h}{2}}^{\frac{h}{2}} \left[\overline{Q_{ij}}\right]\left[g'(z) \quad (g'(z))^2\right] dz \text{ for i, j = 4, 5.} \tag{3.12b}$$

The matrices [*A*], [*B*], [*D*], etc. are symmetric in nature and represent the coupling among virtual field variables. The governing differential equations for a general case may be expressed in the form as follows:

$$f_n = [\Re]\{\Delta_n\} \tag{3.13}$$

where $[\Re]$is operator matrix involving partial differential operators with respect to '*x*' and '*y*', $\{\Delta_n\}$ is the vector containing the field variables while 'f_n' is the force vector. In the present work only cross-ply shells are considered. The cross-ply layers possess reduced coupling effect relative to general layer and the stiffness characteristics of cross-ply sequence are defined as:

$$\begin{aligned} &A_{16} = A_{26} = B_{16} = B_{26} = D_{16} = D_{26} = 0 \\ &E_{16} = E_{26} = F_{16} = F_{26} = H_{16} = H_{26} = 0 \\ &A_{45} = K_{45} = L_{45} = 0 \end{aligned} \tag{3.14}$$

The governing differential equations for cross-ply shells are obtained by substituting the stiffness characteristics as given in Eq. (3.14) in Eq. (3.13). The explicit form of these governing equations are expresses in Eq. (3.15a-e).

$$\begin{aligned} &A_{11}\left(\frac{\partial^2 u_\circ}{\partial x^2} + \frac{1}{R_1}\frac{\partial w_\circ}{\partial x}\right) + B_{11}\left(\Omega\frac{\partial^2 \theta_1}{\partial x^2} - \frac{\partial^3 w_\circ}{\partial x^3}\right) + E_{11}\frac{\partial^2 \theta_1}{\partial x^2} + A_{12}\left(\frac{\partial^2 v_\circ}{\partial x \partial y} + \frac{1}{R_2}\frac{\partial w_\circ}{\partial x}\right) \\ &+ B_{12}\left(\Omega\frac{\partial^2 \theta_2}{\partial x \partial y} - \frac{\partial^3 w_\circ}{\partial x \partial y^2}\right) + E_{12}\frac{\partial^2 \theta_2}{\partial x \partial y} + A_{66}\left(\frac{\partial^2 v_\circ}{\partial x \partial y} + \frac{\partial^2 u_\circ}{\partial y^2}\right) + B_{66}\left(\Omega\frac{\partial^2 \theta_2}{\partial x \partial y} + \Omega\frac{\partial^2 \theta_1}{\partial y^2} - 2\frac{\partial^3 w_\circ}{\partial x \partial y^2}\right) \\ &+ E_{66}\left(\frac{\partial^2 \theta_2}{\partial x \partial y} + \frac{\partial^2 \theta_1}{\partial y^2}\right) = 0 \end{aligned}$$

$$A_{12}\left(\frac{\partial^2 u_\circ}{\partial x\partial y}+\frac{1}{R_1}\frac{\partial w_\circ}{\partial y}\right)+B_{12}\left(\Omega\frac{\partial^2\theta_1}{\partial x\partial y}-\frac{\partial^3 w_\circ}{\partial x^2\partial y}\right)+E_{12}\frac{\partial^2\theta_1}{\partial x\partial y}+A_{22}\left(\frac{\partial^2 v_\circ}{\partial y^2}+\frac{1}{R_2}\frac{\partial w_\circ}{\partial y}\right)$$
$$+B_{22}\left(\Omega\frac{\partial^2\theta_2}{\partial y^2}-\frac{\partial^3 w_\circ}{\partial y^3}\right)+E_{22}\frac{\partial^2\theta_2}{\partial y^2}+A_{66}\left(\frac{\partial^2 v_\circ}{\partial x^2}+\frac{\partial^2 u_\circ}{\partial x\partial y}\right)+B_{66}\left(\Omega\frac{\partial^2\theta_2}{\partial x^2}+\Omega\frac{\partial^2\theta_1}{\partial x\partial y}-2\frac{\partial^3 w_\circ}{\partial x^2\partial y}\right)$$
$$+E_{66}\left(\frac{\partial^2\theta_2}{\partial x^2}+\frac{\partial^2\theta_1}{\partial x\partial y}\right)=0$$

$$A_{11}\left(\frac{1}{R_1}\frac{\partial u_\circ}{\partial x}+\frac{1}{R_1^2}w_\circ\right)+B_{11}\left(\frac{\Omega}{R_1}\frac{\partial\theta_1}{\partial x}-2\frac{1}{R_1}\frac{\partial^2 w_\circ}{\partial x^2}-\frac{\partial^3 u_\circ}{\partial x^3}\right)-D_{11}\left(\Omega\frac{\partial^3\theta_1}{\partial x^3}-\frac{\partial^4 w_\circ}{\partial x^4}\right)+\frac{E_{11}}{R_1}\frac{\partial\theta_1}{\partial x}$$
$$-F_{11}\frac{\partial^3\theta_1}{\partial x^3}+A_{12}\left(\frac{1}{R_1}\frac{\partial v_\circ}{\partial y}+2\frac{1}{R_1R_2}w_\circ+\frac{1}{R_2}\frac{\partial u_\circ}{\partial x}\right)$$
$$+B_{12}\left(\frac{\Omega}{R_1}\frac{\partial\theta_2}{\partial y}+\frac{\Omega}{R_2}\frac{\partial\theta_1}{\partial x}-2\frac{1}{R_1}\frac{\partial^2 w_\circ}{\partial y^2}-2\frac{1}{R_2}\frac{\partial^2 w_\circ}{\partial y^2}-\frac{\partial^3 u_\circ}{\partial x\partial y^2}-\frac{\partial^3 v_\circ}{\partial x^2\partial y}\right)$$
$$-D_{12}\left(\Omega\frac{\partial^3\theta_2}{\partial x^2\partial y}+\Omega\frac{\partial^3\theta_1}{\partial x\partial y^2}-2\frac{\partial^4 w_\circ}{\partial x^2\partial y^2}\right)+E_{12}\left(\frac{1}{R_1}\frac{\partial\theta_2}{\partial y}+\frac{1}{R_2}\frac{\partial\theta_1}{\partial x}\right)-F_{12}\left(\frac{\partial^3\theta_1}{\partial x\partial y^2}+\frac{\partial^3\theta_2}{\partial x^2\partial y}\right)$$
$$+A_{22}\left(\frac{1}{R_2}\frac{\partial v_\circ}{\partial y}+\frac{1}{R_2^2}w_\circ\right)+B_{22}\left(\frac{\Omega}{R_2}\frac{\partial\theta_2}{\partial y}-2\frac{1}{R_2}\frac{\partial^2 w_\circ}{\partial y^2}-\frac{\partial^3 v_\circ}{\partial y^3}\right)-D_{22}\left(\Omega\frac{\partial^3\theta_2}{\partial y^3}-\frac{\partial^4 w_\circ}{\partial y^4}\right)+\frac{E_{22}}{R_2}\frac{\partial\theta_1}{\partial y}$$
$$-F_{22}\frac{\partial^3\theta_2}{\partial y^3}-B_{66}\left(2\frac{\partial^3 v_\circ}{\partial x^2\partial y}+2\frac{\partial^3 u_\circ}{\partial x\partial y^2}\right)-D_{66}\left(2\Omega\frac{\partial^3\theta_1}{\partial x\partial y^2}+2\Omega\frac{\partial^3\theta_2}{\partial x^2\partial y}-4\frac{\partial^3 w_\circ}{\partial x^2\partial y^2}\right)$$
$$-F_{66}\left(2\frac{\partial^2\theta_1}{\partial x\partial y^2}+2\frac{\partial^2\theta_2}{\partial x^2\partial y}\right)+q=0$$

$$B_{11}\left(\Omega\frac{\partial^2 u_\circ}{\partial x}+\frac{\Omega}{R_1}\frac{\partial w_\circ}{\partial x}\right)+D_{11}\left(\Omega^2\frac{\partial^2\theta_1}{\partial x^2}-\Omega\frac{\partial^3 w_\circ}{\partial x^3}\right)+E_{11}\left(\frac{\partial^2 u_\circ}{\partial x^2}+\frac{1}{R_1}\frac{\partial w_\circ}{\partial x}\right)$$
$$+F_{11}\left(2\Omega\frac{\partial^2\theta_1}{\partial x^2}-\frac{\partial^3 w_\circ}{\partial x^3}\right)+H_{11}\left(\frac{\partial^2\theta_1}{\partial x^2}\right)+B_{12}\left(\Omega\frac{\partial^2 v_\circ}{\partial x\partial y}+\frac{\Omega}{R_2}\frac{\partial w_\circ}{\partial x}\right)+D_{12}\left(\Omega^2\frac{\partial^2\theta_2}{\partial y^2}+\Omega\frac{\partial^3 w_\circ}{\partial x\partial y^2}\right)$$
$$+E_{12}\left(\frac{\partial^2 v_\circ}{\partial x\partial y}+\frac{1}{R_2}\frac{\partial w_\circ}{\partial x}\right)+F_{12}\left(2\Omega\frac{\partial^2\theta_2}{\partial x\partial y}-\frac{\partial^3 w_\circ}{\partial x\partial y^2}\right)+H_{12}\left(\frac{\partial^2\theta_2}{\partial x\partial y}\right)+B_{66}\left(\Omega\frac{\partial^2 u_\circ}{\partial y^2}+\Omega\frac{\partial^2 v_\circ}{\partial x\partial y}\right)$$
$$+D_{66}\left(\Omega^2\frac{\partial^2\theta_1}{\partial y^2}+\Omega^2\frac{\partial^2\theta_2}{\partial x\partial y}-2\Omega\frac{\partial^3 w_\circ}{\partial x\partial y^2}\right)+E_{66}\left(\frac{\partial^2 u_\circ}{\partial y^2}+\frac{\partial^2 v_\circ}{\partial x\partial y}\right)+F_{66}\left(2\Omega\frac{\partial\theta_1}{\partial y^2}+2\Omega\frac{\partial^2\theta_2}{\partial x\partial y}-2\frac{\partial^3 w_\circ}{\partial x\partial y^2}\right)$$
$$+H_{66}\left(\frac{\partial^2\theta_1}{\partial y^2}+\frac{\partial^2\theta_2}{\partial x\partial y}\right)-\Omega^2A_{55}\theta_1-2\Omega K_{55}\theta_1-L_{55}\theta_1=0$$

$$B_{12}\left(\Omega\frac{\partial^2 u_\circ}{\partial x\partial y}+\frac{\Omega}{R_1}\frac{\partial w_\circ}{\partial y}\right)+D_{12}\left(\Omega^2\frac{\partial^2\theta_1}{\partial x\partial y}-\Omega\frac{\partial^3 w_\circ}{\partial x^2\partial y}\right)+E_{12}\left(\frac{\partial^2 u_\circ}{\partial x\partial y}+\frac{1}{R_1}\frac{\partial w_\circ}{\partial y}\right)$$
$$+F_{12}\left(2\Omega\frac{\partial^2\theta_1}{\partial x\partial y}-\frac{\partial^3 w_\circ}{\partial x^2\partial y}\right)+H_{12}\left(\frac{\partial^2\theta_1}{\partial x\partial y}\right)+B_{22}\left(\Omega\frac{\partial^2 v_\circ}{\partial y^2}+\frac{\Omega}{R_2}\frac{\partial w_\circ}{\partial y}\right)+D_{22}\left(\Omega^2\frac{\partial^2\theta_2}{\partial y^2}+\Omega\frac{\partial^3 w_\circ}{\partial y^3}\right)$$
$$+E_{22}\left(\frac{\partial^2 v_\circ}{\partial y^2}+\frac{1}{R_2}\frac{\partial w_\circ}{\partial y}\right)+F_{22}\left(2\Omega\frac{\partial^2\theta_2}{\partial y^2}-\frac{\partial^3 w_\circ}{\partial y^3}\right)+H_{22}\left(\frac{\partial^2\theta_2}{\partial y^2}\right)+B_{66}\left(\Omega\frac{\partial^2 u_\circ}{\partial x\partial y}+\Omega\frac{\partial^2 v_\circ}{\partial x^2}\right)$$
$$+D_{66}\left(\Omega^2\frac{\partial^2\theta_1}{\partial x\partial y}+\Omega^2\frac{\partial^2\theta_2}{\partial x^2}-2\Omega\frac{\partial^3 w_\circ}{\partial x^2\partial y}\right)+E_{66}\left(\frac{\partial^2 u_\circ}{\partial x\partial y}+\frac{\partial^2 v_\circ}{\partial x^2}\right)+F_{66}\left(2\Omega\frac{\partial\theta_1}{\partial x\partial y}+2\Omega\frac{\partial^2\theta_2}{\partial x^2}-2\frac{\partial^3 w_\circ}{\partial x\partial y^2}\right)$$
$$+H_{66}\left(\frac{\partial^2\theta_1}{\partial x\partial y}+\frac{\partial^2\theta_2}{\partial x^2}\right)-\Omega^2 A_{44}\theta_2-2\Omega K_{44}\theta_2-L_{44}\theta_2=0$$

(3.15a-3.15e)

The above governing partial differential equations are specifically for symmetric cross-ply laminated composite spherical and cylinder shells. Assuming the suitable solution for field variables ($u_\circ, v_\circ, w_\circ, \theta_1, \theta_2$) and satisfying the necessary boundary conditions; the response of spherical and cylinders shells subjected to desired loading condition is predicted.

3.5.2. Solution Methodology

The governing differential equations as indicated in Eq. (3.15) are solved for simply-supported shells using Navier solution. The associated boundary constraints for simply-supported conditions are indicated in Eq. (3.16).

$$v_\circ = w_\circ = \theta_2 = N_{xx} = M_{xx} = 0 \quad \text{at} \quad x = 0, a.$$
$$u_\circ = w_\circ = \theta_1 = N_{yy} = M_{yy} = 0 \quad \text{at} \quad y = 0, b. \tag{3.16}$$

In the framework of Navier solution, the field variables are assumed in the form series solution as mentioned in Eq. (3.17).

$$u_\circ = \sum_{m=1}^{\infty}\sum_{n=1}^{\infty} U_{mn}\cos(\alpha x)\sin(\beta y)$$
$$v_\circ = \sum_{m=1}^{\infty}\sum_{n=1}^{\infty} V_{mn}\sin(\alpha x)\cos(\beta y)$$
$$w_\circ = \sum_{m=1}^{\infty}\sum_{n=1}^{\infty} W_{mn}\sin(\alpha x)\sin(\beta y) \tag{3.17a-3.17e}$$
$$\theta_1 = \sum_{m=1}^{\infty}\sum_{n=1}^{\infty} X_{mn}\cos(\alpha x)\sin(\beta y)$$
$$\theta_2 = \sum_{m=1}^{\infty}\sum_{n=1}^{\infty} Y_{mn}\sin(\alpha x)\cos(\beta y)$$

$$\alpha = \frac{m\pi}{a}, \quad \beta = \frac{n\pi}{b}$$

The above assumed solution inherently satisfy the associated boundary condition Eq. (3.16). Also, the transverse loads are assumed in the form similar to that of transverse deflection and given in Eq. (3.18)

$$q = \sum_{m=1}^{\infty}\sum_{n=1}^{\infty} q_{mn} \sin(\alpha x)\sin(\beta y) \tag{3.18a}$$

where $q_{mn} = q_\circ$ for sinusoidal load

$q_{mn} = 16q_\circ / \pi^2 mn$ for uniformly distributed load

$q_{mn} = 4q_\circ / ab \times \sin(\varsigma m/a)\sin(\eta n/b)$ for point load.

The assumed solution and loading are substituted in the governing differential equation given by Eq. (3.15). The simplification of these equations yield five simultaneous equations and may be expressed in the form as follows:

$$[R]_{5\times5}\{\Delta\}_{5\times1} = \{F\}_{5\times1} \tag{3.19}$$

where $\{\Delta\}^T$ is a vector containing arbitrary coefficients and $\{F\}^T$ is the force vector. The terms of stiffness matrix [*R*] are indicated in Appendix A. The arbitrary coefficient are obtained by solving Eq. (3.19) which are further substituted in Eq. (3.17) to yield the mid-plane displacements and rotations. The strain and stresses are obtained by implemented strain-displacement relation Eq. (3.3) and stress-strain relations Eq. (3.6) respectively.

3.6. Finite element formulation and implementation:

The Navier-type Close form solution only give exact solution for simply supported boundary condition. To overcome this limitation and study the shell structure for other boundary condition (Clamped, angle-ply), a Finite element approach is used to investigate the bending behaviour of the laminated composite cross-ply laminated square shell. The formulation for Finite element method is discussed in this section. The problem of C_1 continuity associated with higher order theory is overcome by introducing two more independent variable in displacement field relation $\varphi_1 = \partial w/a_1\partial\xi_1$ and $\varphi_2 = \partial w/a_2\partial\xi_2$. The displacement field relation with insured C_0 continuity as shown below:

$$\begin{aligned} u(\xi_1,\xi_2,\zeta) &= \left(1+\frac{\zeta}{R_1}\right)u_\circ - \zeta\varphi_1 + (g(\zeta)+\Omega\zeta)\theta_1 \\ v(\xi_1,\xi_2,\zeta) &= \left(1+\frac{\zeta}{R_2}\right)u_\circ - \zeta\varphi_2 + (g(\zeta)+\Omega\zeta)\theta_2 \\ w(\xi_1,\xi_2,\zeta) &= w_\circ \end{aligned} \tag{3.20}$$

The displacement relation is implemented in strain displacement relation given in Eq. (3.2) and rewrite in terms of generalised strain as shown below

$$\begin{aligned}
\varepsilon_1 &= \varepsilon_1^0 + \varepsilon_1^1 + z\kappa_1^0 + g(z)\kappa_1^1 \\
\varepsilon_2 &= \varepsilon_2^0 + \varepsilon_2^1 + z\kappa_2^0 + g(z)\kappa_2^1 \\
\varepsilon_6 &= \varepsilon_6^0 + z\kappa_6^0 + g(z)\kappa_6^1 \\
\varepsilon_4 &= \varepsilon_4^0 + g'(z)\kappa_4^2 + \Omega\kappa_4^2 \\
\varepsilon_5 &= \varepsilon_5^0 + g'(z)\kappa_5^2 + \Omega\kappa_5^2
\end{aligned} \tag{3.21}$$

Whereas,

$$\varepsilon_1^0 = \frac{\partial u_\circ}{\partial x}, \quad \kappa_1^0 = \Omega\frac{\partial \theta_1}{\partial x} - \frac{\partial \phi_1}{\partial x}, \quad \varepsilon_1^1 = \frac{w_\circ}{R_1}, \kappa_1^1 = \frac{\partial \theta_1}{\partial x}$$

$$\varepsilon_2^0 = \frac{\partial v_\circ}{\partial y}, \quad \kappa_2^0 = \Omega\frac{\partial \theta_2}{\partial y} - \frac{\partial \phi_2}{\partial y}, \quad \varepsilon_2^1 = \frac{w_\circ}{R_2}, \kappa_2^1 = \frac{\partial \theta_2}{\partial y}$$

$$\varepsilon_6^0 = \frac{\partial v_\circ}{\partial x} + \frac{\partial u_\circ}{\partial y}, \quad \kappa_6^0 = \Omega\left(\frac{\partial \theta_1}{\partial y} + \frac{\partial \theta_2}{\partial x}\right) - \left(\frac{\partial \phi_1}{\partial y} + \frac{\partial \phi_2}{\partial x}\right), \kappa_6^1 = \left(\frac{\partial \theta_1}{\partial y} + \frac{\partial \theta_2}{\partial x}\right)$$

$$\varepsilon_4^0 = \frac{\partial w_\circ}{\partial y} - \phi_y, \kappa_4^2 = \theta_2$$

$$\varepsilon_5^0 = \frac{\partial w_\circ}{\partial x} - \phi_x, \kappa_5^2 = \theta_1$$

3.6.1. Element Selection:

An eight noded quadratic element with C_0 continuity is used to discretise the square shell structure in sub-domains. An element have seven degree of freedom per node. The shape function on k node for a quadratic element are as shown follows:

$$N_i = \begin{cases} \frac{1}{4}(1+\xi\xi_i)(1+\eta\eta_i)(\xi\xi_i + \eta\eta_i - 1) & \text{for} \quad i = 1,2,3,4 \\ \frac{1}{2}(1-\xi^2)(1+\eta\eta_i) & \text{for} \quad i = 5,7 \\ \frac{1}{2}(1-\eta^2)(1+\xi\xi_i) & \text{for} \quad i = 6,8 \end{cases} \tag{3.22}$$

Further, the field variables expressed in terms of shape function are represented as:

$$l = \sum_{i=1}^{8} N_i l_i \text{ and } q = \sum_{i=1}^{8} N_i q_i \tag{3.23}$$

where l is the generalised geometrical co-ordinates, l_i represent the geometrical position of ith node of the element and q is the generalised field variable, q_i represent the field variables at ith node of the element.

3.6.2. Derivation of Strain Energy

The representation of strain vector in terms of generalized strain terms:

$$\{\varepsilon\}_{5\times1} = [H]_{5\times15}\{\bar{\varepsilon}\}_{15\times1} \tag{3.24}$$

where $\{\bar{\varepsilon}\}$ is the generalised strain vector and $[H]$ matrix contain the coefficients of generalised strain parameters.

$$\{\bar{\varepsilon}\}_{15\times1} = \{\varepsilon_1^0 \quad \varepsilon_2^0 \quad \varepsilon_6^0 \quad \varepsilon_4^0 \quad \varepsilon_5^0 \quad \varepsilon_1^1 \quad \varepsilon_2^1 \quad \kappa_1^0 \quad \kappa_2^0 \quad \kappa_6^0 \quad \kappa_4^0 \quad \kappa_5^0 \quad \kappa_1^1 \quad \kappa_2^1 \quad \kappa_6^1\}$$

and

$$[H] = \begin{bmatrix} 1 & 0 & 0 & 1 & 0 & z & 0 & 0 & g(z) & 0 & 0 & 0 & 0 & 0 & 0 \\ 0 & 1 & 0 & 0 & 1 & 0 & z & 0 & 0 & g(z) & 0 & 0 & 0 & 0 & 0 \\ 0 & 0 & 1 & 0 & 0 & 0 & 0 & z & 0 & 0 & g(z) & 0 & 0 & 0 & 0 \\ 0 & 0 & 0 & 0 & 0 & 0 & 0 & 0 & 0 & 0 & 0 & 1 & 0 & g'(z) & 0 \\ 0 & 0 & 0 & 0 & 0 & 0 & 0 & 0 & 0 & 0 & 0 & 0 & 1 & 0 & g'(z) \end{bmatrix}$$

Further, the generalized strain is expressed in terms of seven independent field variables as shows below:

$$\{\bar{\varepsilon}\}_{15\times1} = [L]_{15\times7}\{q\}_{7\times1} \tag{3.25}$$

Where $\{q\}_{7\times1} = [u_\circ \quad v_\circ \quad w_\circ \quad \phi_1 \quad \phi_2 \quad \theta_1 \quad \theta_2]^T$

By implement Eq (3.23) and Eq (3.25), the strain displacement relation can be expressed as for l^{th} node:

$$\{\bar{\varepsilon}_i\}_l = \{B\}_l\{q\}_l \tag{3.26}$$

The strain energy due to the strains for the nth element can be obtained using the Eq. (3.24) and (3.26) along with the constitutive relations as follows:

$$U^{(l)} = \frac{1}{2}\int_V \{\varepsilon\}_l^T\{\sigma\}dV = \frac{1}{2}\int_V \{\varepsilon\}_l^T\{\bar{Q}_{il}\}\{\varepsilon\}_l dV = \frac{1}{2}\int_V \{\varepsilon_i\}_l^T\{H\}_l^T\{\bar{Q}_{il}\}\{H\}_l\{\varepsilon_i\}_l dV$$

$$= \frac{1}{2}\int_S \{q\}_l^T \{B\}_l^T \{D\}_l \{B\}_l \{q\}_l dxdy = \frac{1}{2}\int_S \{q\}_l^T \{K\}_l \{q\}_l dxdy \tag{3.27}$$

By performing assembling for total number of elements (*NL*), the total strain energy (U_T) can be obtained as follows:

$$U_T = \sum_{l=1}^{NL} U^{(l)} = \frac{1}{2}\{q\}^T \{K\}\{q\} \tag{3.28}$$

where $\{K\}$ is the global Stiffness matrix appear due to artificial constraints and *q* matrix is generalized field variables .

3.6.3.Work done due to transverse load

The total work done (*W*) due to transverse load is obtained as:

$$W = \sum_{l=1}^{NL} W_l^{(e)} = \sum_{l=1}^{NL} \{f^{(e)}\}_l \{q\}_l + \sum_{l=1}^{NL} \{B\}_l^T \{D^{th}\}_l \{q\} \tag{3.29}$$

where $W^{(e)}$ are external work done due to transverse. The matrix $\{D\}$ is the material matrix which is function of material properties and expressed as $D^{th} = \int H_l^T \{\overline{Q}_{il}\}\{\varepsilon^{Th}\}_l dz$ and $\{f\} = \{0\ 0\ q_o\ 0\ 0\ 0\ 0\ 0\}$ and q_o is the transverse load applied on to the laminated composite shell, for sinusoidal load $q_\circ = q_\circ \sin(\pi x/a)\sin(\pi y/b)$ and for UDL $q_\circ = q_\circ$.

3.7. Summary

The modelling of laminated composite shell in the framework of analytical and finite element is shown. The governing differential equation are solved analytically for simply supported boundary condition and solved by using Navier-type close form solution. Moreover a Finite element model is also developed for various boundary conditions like SSSS, SCSS, SCSC, and CCCC.

4.1. Introduction:

The algorithm of the developed mathematical formulation and solution methodology is implemented in MATLAB and a generalized computer program is developed. The developed computer code is capable to predict the bending behavior of simply supported cross ply multi-layered composite shells. In this section, extensive examples of shell structures under different transverse loadings are considered and the response is predicted in terms of transverse deflection and stresses. The obtained results are compared with the existing results and on the basis of comparison, the validity, applicability and accuracy of IHSDT for multi-layered shells is ensured. In this section the material properties (MP1) of each layer of laminated shells are given as follow [Reddy et al. (1985)]:

$$E_1 = E_3 = 25E_2;\ G_{12} = G_{13} = 0.5E_2;\ G_{23} = 0.2E_2;\ \nu_{12} = \nu_{13} = 0.25;$$

The non-dimensional results for transverse centre deflection and stresses are presented with the following generalized non-dimensional forms:

$$\overline{w} = w_\circ\left(\frac{a}{2},\frac{b}{2}\right)\left(\frac{1000E_2h^3}{b^4q_\circ}\right);\ \overline{\sigma_{xx}} = \sigma_{xx}\left(\frac{a}{2},\frac{b}{2},\frac{h}{2}\right)\frac{h^2}{q_\circ a^2};$$

$$\overline{\tau_{xy}} = \tau_{xy}\left(0,0,\frac{h}{2}\right)\frac{h^2}{q_\circ a^2};\ \overline{\tau_{xz}} = \tau_{xz}\left(0,\frac{b}{2},0\right)\frac{h}{q_\circ a};\ \overline{\tau_{yz}} = \tau_{yz}\left(\frac{a}{2},0,0\right)\frac{h}{q_\circ a}$$

4.2. Static analysis of laminated composite shell using close-form solution.

4.2.1. Multi-layered spherical and cylindrical shells under sinusoidal transverse load.

A three layered symmetric cross-ply shell with lamination sequence [0/90/0] subjected to sinusoidal load (SSL) is considered. The bending behavior is examined for a moderately thick shallow shell with a/h =10, $a = b$ and R/a ranging from 5 to 50. Also, the behavior of plate is examined as a special case of $R/a = \infty$. The obtained transverse deformation and stresses are indicated in Table 1 along with the results due to other equivalent layer theories such as ED1, ED2, ED4, ED2D, ED4D by Carrera et al. (2011) whereas FSDT and HSDT by Reddy et al. (1985), and TSDT by Mantari et al. (2011). To the author's belief, the exact three-dimensional (3D) results for the considered problem are not known in the literature. However, the results due to layer wise theory by Carrera et al. (2011) are available believed to be most accurate in the existing literature.

Table 4.1: Non-dimensional central deflection and stresses of cross ply square three layered [0/90/0] for a/h = 10 under SSL.

R/a	Theory	$\bar{w}\left(\frac{a}{2},\frac{b}{2}\right)$		$\bar{\sigma}_{xx}\left(\frac{a}{2},\frac{b}{2},\frac{h}{2}\right)$		$\bar{\sigma}_{xy}\left(0,0,\frac{h}{2}\right)$		$\bar{\sigma}_{xz}\left(0,\frac{b}{2},0\right)$	
			% Diff	*10	% Diff	* -100	% Diff	* 100	%Diff
5	Present	6.9522	-4.92	5.7322	-1.22	1.4288	0.37	2.9326	-15.21
	LM4[a]	7.3120	0.00	5.8032	-	1.4235	-	3.4588	0.00
	ED1[a]	6.1844	-15.42	-	-	-	-	1.3144	-62.00
	ED2[a]	-	-	5.1496	-11.26	1.2380	-13.03	-	-
	ED4[a]	6.9573	-4.85	5.7757	-0.47	1.4066	-1.19	2.5088	-27.47
	ED2D[a]	6.1904	-15.34	5.1828	-10.69	1.2617	-11.37	1.3149	-61.98
	ED4D[a]	7.0014	-4.25	5.8194	0.28	1.4375	0.98	2.5198	-27.15
	FSDT[b]	6.4253	-12.13	5.1932	-10.51	1.2522	-12.03	1.3146	-61.99
	TSDT[c]	6.8853	-5.84	-	-	-	-	-	-
	HSDT[b]	6.7688	-7.43	-	-	-	-	-	-
10	Present	7.2307	-3.56	5.8645	-0.87	2.1536	-0.16	3.0501	-14.24
	LM4[a]	7.4978	0.00	5.9161	-	2.1570	-	3.5564	0.00
	ED1[a]	6.3030	-15.94	-	-	-	-	1.3565	-61.86
	ED2[a]	-	-	5.2059	-12.00	1.8431	-14.55	-	-
	ED4[a]	7.1230	-5.00	5.8630	-0.90	2.0992	-2.68	2.5904	-27.16
	ED2D[a]	6.3074	-15.88	5.2323	-11.56	1.8714	-13.24	1.3569	-61.85
	ED4D[a]	7.1661	-4.42	5.9037	-0.21	2.1367	-0.94	2.6015	-26.85
	FSDT[b]	6.6247	-11.64	5.2379	-11.46	1.8666	-13.46	1.3568	-61.85
	TSDT[c]	7.1583	-4.53	-	-	-	-	-	-
	HSDT[b]	7.0325	-6.21	-	-	-	-	-	-
20	Present	7.3038	-2.99	5.8747	-0.74	2.5125	3.05	3.0810	-13.77
	LM4[a]	7.5290	-	5.9187	-	2.4382	-	3.5732	0.00
	ED1[a]	6.3195	-16.06	-	-	-	-	1.3674	-61.73
	ED2[a]	-	-	5.1938	-12.25	1.8431	-24.41	-	-
	ED4[a]	7.1499	-5.04	5.8554	-1.07	2.0992	-13.90	2.6090	-26.98
	ED2D[a]	6.3220	-16.03	5.2164	-11.87	2.1698	-11.01	1.3676	-61.73
	ED4D[a]	7.1911	-4.49	5.8936	-0.42	2.4785	1.65	2.6200	-26.68
	FSDT[b]	6.6756	-11.33	5.2192	-11.82	2.1674	-11.11	1.3676	-61.73
	TSDT[c]	7.2299	-3.97	-	-	-	-	-	-
	HSDT[b]	7.1016	-5.68	-	-	-	-	-	-
50	Present	7.3245	-2.69	5.8618	-0.68	2.7225	-0.14	3.0897	-13.51
	LM4[a]	7.5267	0.00	5.9021	-	2.7264	-	3.5724	0.00
	ED1[a]	6.3149	-16.10	-	-	-	-	1.3709	-61.63
	ED2[a]	-	-	5.1734	-12.35	2.3133	-15.15	-	-
	ED4[a]	7.1472	-5.04	5.8338	-1.16	2.6363	-3.30	2.6127	-26.86
	ED2D[a]	6.3160	-16.09	5.1934	-12.01	2.3442	-14.02	1.3705	-61.64
	ED4D[a]	7.1867	-4.52	5.8701	-0.54	2.6777	-1.79	2.6234	-26.56
	FSDT[b]	6.6902	-11.11	5.1841	-12.17	2.4009	-11.94	1.3709	-61.63
	TSDT[c]	7.2502	-3.67	-	-	-	-	-	-
	HSDT[b]	7.1212	-5.39	-	-	-	-	-	-
Plate	Present	7.3285	2.86	5.8452	-0.65	2.8593	-0.12	3.0914	-13.34
	Pagano[d]	-	-	5.8836	-	2.8628	-	3.5674	0.00
	LM4[a]	7.1250	-	5.8836	0.00	2.8628	0.00	3.5674	0.00
	ED4 [a]	7.1374	0.17	5.8122	-1.21	2.7651	-3.41	2.6119	-26.78
	ED2[a]	-	-	5.1542	-	2.4266	-15.24	-	-
	ED1[a]	-	-	-	-	-	-	1.3710	-61.57
	ED4D[a]	7.1757	0.71	5.8473	-0.62	2.8072	-1.94	2.6225	-26.49
	ED2D[a]	6.3059	-11.50	5.1725	-12.09	2.4580	-14.14	1.3710	-61.57
	HSDT[b]	7.1250	0	-	-	-	-	-	-
	FSDT[b]	6.6939	-6.05	5.1725	-	2.4580	-14.14	1.3710	-

[a] Carrera et al. (2011); [b] Reddy et al. (1985); [c] Mantari et al. (2011); [d] N.J Pagano (1970)

Therefore, the comparison of the results is presented with layer wise model 4 (LM4) model presented by *Carrera* et al. (2011). It is observed that the average percentage difference for the transverse deformation by IHSDT is about 2.26 % relative to 15.88 % by ED1, 4.02 % by ED4, 14.97 % by ED2D, 3.678% by ED4D, 10.452% by FSDT, 4.942 % by HSDT, and 4.502 % by TSDT.

Table 4.2: Non-dimensional central deflection and stresses of cross ply square three layered [0/90/0] for a/h = 100 under SSL.

R/a	Theory	$\bar{w}\left(\frac{a}{2},\frac{b}{2}\right)$	$\bar{\sigma}_{xx}\left(\frac{a}{2},\frac{b}{2},\frac{h}{2}\right)$	$\bar{\sigma}_{xz}\left(0,\frac{b}{2},0\right)$	$\bar{\sigma}_{yz}\left(\frac{a}{2},0,0\right)$
5	Present	1.0323	1.5589	0.7863	1.9320
	LM4[a]	1.0364	1.5570	0.9373	1.9678
	ED1[a]	1.0383	1.5668	0.2944	0.3132
	ED4[a]	1.0361	1.5586	0.6234	0.6633
	ED2D[a]	1.0355	-	-	-
	FSDT[b]	1.0337	1.5596	0.2937	0.3132
	TSDT [c]	1.0328	-	-	-
	HSDT[b]	1.0321	-	-	-
10	Present	2.4107	3.3161	1.8363	4.5119
	LM4[a]	2.4166	-	-	-
	ED1[a]	2.4158	-	-	-
	ED4 [a]	2.4150	-	-	-
	ED2D[a]	2.4120	-	-	-
	FSDT[b]	2.4109	-	-	-
	TSDT[c]	2.4132	-	-	-
	HSDT[b]	2.4099	-	-	-
20	Present	3.6188	4.7345	2.7565	6.7730
	LM4[a]	3.6329	4.7360	3.2893	6.9032
	ED1[a]	3.6160	4.7381	1.1434	3.9376
	ED4 [a]	3.6206	4.7366	2.3011	5.1734
	ED2D[a]	3.6140	-	-	-
	FSDT[b]	3.6150	4.7325	1.1428	3.9376
	TSDT[c]	3.6242			
	HSDT[b]	3.6170	-	-	-
50	Present	4.2095	5.3373	3.2064	7.8785
	LM4[a]	4.2130	-	-	-
	ED1[a]	4.2001	-	-	-
	ED4 [a]	4.2086	-	-	-
	ED2D[a]	4.1997	-	-	-
	FSDT[b]	4.2027	-	-	-
	TSDT[c]	4.2166	-	-	-
	HSDT[b]	4.2071	-	-	-
Plate	Present	4.3445	5.3916	3.3093	8.1313
	Pagano[d]	4.3471	5.3923	3.9468	8.2828
	LM4[a]	4.3471	5.3923	3.9468	8.2828
	ED1[a]	4.3329	5.3845	1.4159	5.8559
	ED4 [a]	4.3424	5.3914	2.8061	7.3450
	ED2D[a]	4.3329	-	-	-
	FSDT[b]	4.3370	5.3846	1.4159	5.8559
	TSDT[c]	4.3521	-	-	-
	HSDT[b]	4.3420	-	-	-

[a] Carrera et al. (2011); [b] Reddy et al. (1985); [c] Mantari et al. (2011); [d] N.J Pagano (1970)

Also, the applicability and accuracy of IHSDT for the evaluation of stresses is evident from the data obtained. In order to examine the bending characteristics of thin shell, a three layered symmetric cross-ply shell with lamination sequence [0/90/0] subjected to SSL is considered. The bending analysis is performed for the thin shell with a/h =100 and behavior is examined in terms of transverse deflection and stresses. The obtained results are indicated in Table 2 along with the existing results. The radius of curvature to span ratio (R/a) is varied as 5, 10, 20, 50, and ∞.

Table 4.3: Non-dimensional central deflection of cross ply square with stacking sequence [0/90] and [0/90/90/0] under the effect SSL.

R/a	Theory	0°/90°		0°/90°/90°/0°	
		a/h=10	a/h=100	a/h=10	a/h=100
5	Present	11.0382	1.1937	6.9098	1.0265
	FSDT[a]	11.1660	1.1948	6.3623	1.0279
	TSDT [b]	11.1080	1.1940	-	-
	HSDT [a]	11.1660	1.1937	6.7865	1.0264
10	Present	11.7504	3.5732	7.1869	2.4029
	FSDT[a]	12.1230	3.5760	6.5595	2.403
	TSDT [b]	11.8296	3.5751	-	-
	HSDT [a]	11.8960	3.5733	7.0536	2.4024
20	Present	11.9431	7.1229	7.2597	3.6145
	FSDT[a]	12.3090	7.1270	6.6099	3.6104
	TSDT [b]	12.0249	7.1295	-	-
	HSDT [a]	12.0940	7.1236	7.1237	3.6133
50	Present	11.9982	9.8679	7.2803	4.2087
	FSDT[a]	12.3620	9.8717	6.6244	4.2015
	TSDT [b]	12.0807	9.8800	-	-
	HSDT [a]	12.1500	9.8692	7.1436	4.2071
100	Present	12.0061	10.4428	-	-
	FSDT[a]	12.3730	10.4460	7.1464	4.3082
	TSDT [b]	12.0914	10.4562	-	-
	HSDT [a]	12.1610	10.4440	7.2833	4.3099
Plate	Present	12.0087	10.6496	7.2843	4.3447
	Pagano[c]	-	-	7.4300	4.390
	FSDT[a]	12.3730	10.6530	6.628	4.3368
	TSDT [b]	12.0914	10.6635	-	-
	HSDT [a]	12.1610	10.6510	7.1474	4.343

[a] Readdy et al. (1985); [b] Mantari et al. (2011); [c] Pagano N.J (1970)

Further, the bending characteristics of anti-symmetric and symmetric cross-ply shells are examined in terms of maximum non-dimensional transverse deflection. For anti-symmetric laminate, a two layered shell with lamination sequence [0/90] is considered while the lamination sequence as [0/90/90/0] is considered for the symmetric configuration. The MP1 material properties are assumed for each layer and each layer possess equal thickness. The bending results are obtained for thin (a/h =100) and thick (a/h = 10) shells for a variety of

radius of curvature to span ratio (R/a) ranging from 5 to 50. The results for the plate are also examined as a special case for $R/a = \infty$. The obtained results are indicated in Table 4.3 along with the existing results due to TSDT by Mantari et al. (2011), HSDT and FSDT by Reddy et al. (1985). The agreement of the present results with the existing results is evident from the data presented in the table. It is observed that the non-dimensional deflection for the thin shells is lower than that of the thick shell for both the configurations. Moreover, the increment in radius of curvature increases the non-dimensional deflection thereby establishing that the non-dimensional deflection is inversely proportional to the curvature of the shell.

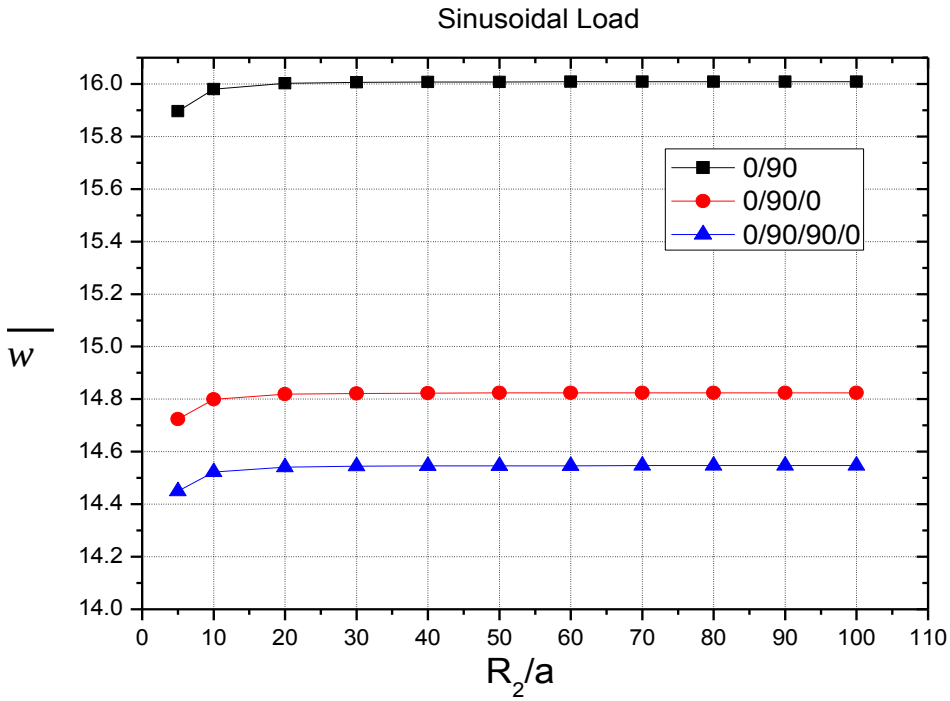

Figure 4.1: Transverse central deflection, with parametric variation of R_2/a, of a symmetric and anti-symmetric cross-ply laminated composite cylindrical shell under the effect of sinusoidal load.

It should be noted that the above discussed examples are for the doubly curved shells ($R_1 = R_2 = R$). In order to examine the response of cylindrical shells ($R_1 = \infty$, $R_2 = R$), a two layered anti-symmetric [0/90], a three layered symmetric [0/90/0], and a four layered symmetric [0/90/90/0] laminated shells are considered. The response of these cylindrical shells by varying the R/a ratio and span-thickness ratio (a/h). The effect of varying R/a ratio on non-dimensional deflection of laminated shells (a/h =5) subjected to SSL is shown in Fig. 4.1. In the analysis, R/a ratio is varied from 5 to 100. It is observed that the non-dimensional deflection increases

with increase in R/a ratio. Also, this increment is noticeable till R/a =20, further the non-dimensional deflection increases marginally.

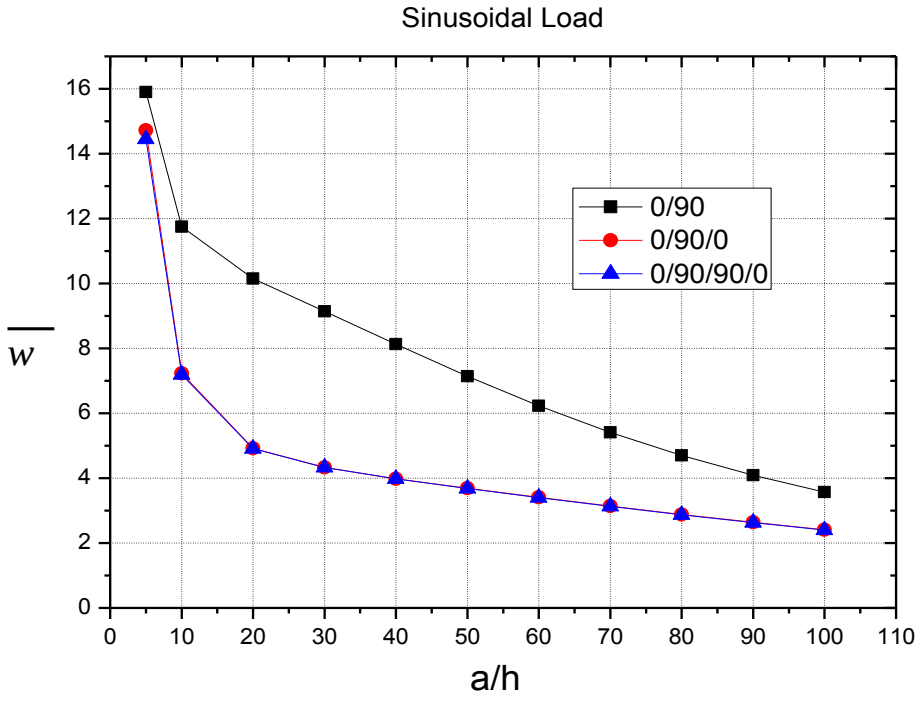

Figure 4.2: Transverse central deflection, with parametric variation of R_2/a, of a symmetric and anti-symmetric cross-ply laminated composite cylindrical shell under the effect of sinusoidal load.

The effect of span-thickness ratio on non-dimensional deflection of cylindrical shells is indicated in Fig. 4.2. It is observed that the non-dimensional deflection increases with increase in a/h ratio. Moreover, the behavior of symmetric laminates with three layered and four layered lamination sequence are predicted to be similar.

4.2.2. Multi-layered spherical and cylindrical shells under uniformly distributed transverse load.

In order to examine the bending response for non-dimensional transverse deflection and stresses under uniform distributed load (UDL) over the variation of R/a ranging from 5 to 50 , a moderately thick shallow (a/h=10) three layered symmetric cross-ply square laminated composite spherical shell is considered. The special case of spherical shell, plate ($R_1=R_2=\infty$) also examined. The Navier-type close form solution are used to solve the governing equation with $\bar{m}$ and $\bar{n}$ in Eq. (4.17) equal to 13 is used.

Table 4.4: Non-dimensional central deflection and stresses of cross ply square three layered [0/90/0] for a/h = 10 under UDL.

R/a	Theory	$\bar{w}\left(\frac{a}{2},\frac{b}{2}\right)$		$\bar{\sigma}_{xx}\left(\frac{a}{2},\frac{b}{2},\frac{h}{2}\right)$		$\bar{\sigma}_{xz}\left(0,\frac{b}{2},0\right)$	
			% Diff		% Diff		% Diff
5	Present	10.6241	-5.07	8.3862	-1.48	6.7485	10.15
	LM4[a]	11.1910	0.00	8.5121	0.00	6.1266	0.00
	ED1[a]	-	-	7.7557	-8.89	2.4598	-59.85
	ED4[a]	10.6400	-4.92	8.4697	-0.50	4.5157	-26.29
	ED2D[a]	-	-	7.7474	-8.98	2.4611	-59.83
	ED4D[a]	10.6950	-4.43	8.5298	0.21	4.5566	-25.63
	FSDT[b]	9.7937	-12.49	7.7606	-8.83	2.4606	-59.84
	TSDT [c]	10.5169	-6.02	-	-	-	-
	HSDT[b]	10.3320	-7.68	-	-	-	-
10	Present	11.0677	-3.68	8.6174	-	6.9508	-
	LM4[a]	11.4910	0.00	-	-	-	-
	ED1[a]	-	-	-	-	-	-
	ED4 [a]	-	-	-	-	-	-
	ED2D[a]	-	-	-	-	-	-
	ED4D[a]	10.6950	-6.93	-	-	-	-
	FSDT[b]	10.1100	-12.02	-	-	-	-
	TSDT [c]	10.9516	-4.69	-	-		-
	HSDT[b]	10.7520	-6.43	-	-	-	-
20	Present	11.1843	-3.10	8.6446	-0.94	7.0038	11.10
	LM4[a]	11.5420	0.00	8.7268	0.00	6.3042	0.00
	ED1[a]	-	-	7.8284	-10.29	2.5415	-59.69
	ED4[a]	10.9510	-5.12	8.6283	-1.13	4.6738	-25.86
	ED2D[a]	-	-	7.8340	-10.23	2.5419	-59.68
	ED4D[a]	11.0030	-4.67	8.6829	-0.50	4.7127	-25.25
	FSDT[b]	10.1910	-11.71	7.8376	-10.19	2.5419	-59.68
	TSDT [c]	11.0658	-4.13	-	-	-	-
	HSDT[b]	10.8620	-5.89	-	-	-	-
50	Present	11.2173	-2.80	8.6310	-	7.0188	-
	LM4[a]	11.5400	0.00	-	-	-	-
	ED1[a]	-	-	-	-	-	-
	ED4[a]	11.0130	-4.57	-	-	-	-
	ED2D[a]	-	-	-	-	-	-
	ED4D[a]	10.9970	-4.71	-	-	-	-
	FSDT[b]	10.2140	-11.49	-	-	-	-
	TSDT [c]	11.0982	-3.83	-	-	-	-
	HSDT[b]	10.8930	-5.61	-	-	-	-
Plate	Present	11.2237	-2.61	8.6092	-0.86	7.0217	11.78
	Pagano[d]	11.5250	0.00	8.6842	0.00	6.2815	0.00
	LM4[a]	11.5240	-0.01	8.6820	-0.03	6.2926	0.18
	ED1[a]	-		7.7658	-10.58	2.5462	-59.47
	ED4[a]	10.9330	-5.14	8.5709	-1.30	4.6772	-25.54
	ED2D[a]	-	-	7.7757	-10.46	2.5462	-59.47
	ED4D[a]	10.9810	-4.72	8.6219	-0.72	4.7149	-24.94
	FSDT[b]	10.2200	-11.32	7.7757	-10.46	2.5462	-59.47
	TSDT [c]	11.1044	-3.65	-	-	-	-
	HSDT[b]	10.8990	-5.43	-	-	-	-

[a] Carrera et al. (2011); [b] Reddy et al. (1985); [c] Mantari et al. (2011); [d] N.J Pagano (1970)

Table 4.5: Non-dimensional central deflection and stresses of cross ply square three layered [0/90/0] for a/h = 100 under UDL.

R/a	Theory	$\bar{w}\left(\frac{a}{2},\frac{b}{2}\right)$	$\bar{\sigma}_{xx}\left(\frac{a}{2},\frac{b}{2},\frac{h}{2}\right)$	$\bar{\sigma}_{xz}\left(0,\frac{b}{2},0\right)$	$\bar{\sigma}_{yz}\left(\frac{a}{2},0,0\right)$
5	Present	1.5094	1.9762	3.4704	3.0283
	LM4[a]	1.5155	1.9719	2.4751	1.9984
	ED1[a]	-	1.9869	0.8356	0.9622
	ED4[a]	1.5152	1.9742	1.7070	1.3541
	ED2D[a]	-	1.9766	0.8345	0.9610
	ED4D[a]	1.5151	1.9747	1.7072	1.3544
	FSDT[b]	1.5118	1.9767	0.8344	0.9611
	TSDT [c]	1.5101	-	-	-
	HSDT[b]	1.5092	-	-	-
10	Present	3.6439	4.6919	5.3468	4.6844
	LM4[a]	3.6528	-	-	-
	ED1[a]	-	-	-	-
	ED4[a]	3.6507	-	-	-
	ED2D[a]	-	-	-	-
	ED4D[a]	3.6507	-	-	-
	FSDT[b]	3.6445	-	-	-
	TSDT [c]	3.6476	-	-	-
	HSDT[b]	3.6426	-	-	-
20	Present	5.5531	6.9706	6.8752	5.7235
	LM4[a]	5.5610	6.9720	6.1677	3.5590
	ED1[a]	-	6.9771	2.1692	2.0300
	ED4[a]	5.5560	6.9734	4.3429	2.7167
	ED2D[a]	-	6.9681	2.1682	2.0294
	ED4D[a]	5.5562	6.9736	4.3429	2.7174
	FSDT[b]	5.5459	6.9682	2.1682	2.0295
	TSDT [c]	5.5614	-	-	-
	HSDT[b]	5.5503	-	-	-
50	Present	6.4933	7.9678	7.6127	6.1614
	LM4[a]	6.4988	-	-	-
	ED1[a]	-	-	-	-
	ED4[a]	6.4921	-	-	-
	ED2D[a]	-	-	-	-
	ED4D[a]	6.4924	-	-	-
	FSDT[b]	6.4827	-	-	-
	TSDT [c]	6.5045	-	-	-
	HSDT[b]	6.4895	-	-	-
Plate	Present	6.7087	8.0838	7.7809	6.2567
	Pagano[d]	6.7127	8.0831	7.2115	3.8787
	LM4[a]	6.7127	8.0839	7.2116	3.8789
	ED1[a]	-	8.0735	2.6012	2.4255
	ED4[a]	6.7055	8.0830	5.1443	3.1725
	ED2D[a]	-	8.0736	2.6012	2.4255
	ED4D[a]	6.7058	8.0830	5.1443	3.1733
	FSDT[b]	6.6970	8.0736	2.6012	2.4255
	TSDT [c]	6.7206	-	-	-
	HSDT[b]	6.7047	-	-	-

[a] Carrera et al. (2011); [b] Reddy et al. (1985); [c] Mantari et al. (2011); [d] N.J Pagano (1970)

In Table 4.4, the response for non-dimensional deflection and stresses is presented along with the results due to other equivalent layer theories such as ED1, ED2, ED4, ED2D, ED4D by Carrera et al. (2011) where as FSDT and HSDT by Reddy et al. (1985), and TSDT by Mantari et al. (2011).The results are compared with results represented by layer-wise

theory LM4 model presented by *Carrera* et al. (2011). It is observed that the average percentage difference for the transverse deformation by IHSDT is about 3.452 % relative to 4.937 % by ED4, 5.092 % by ED4D, 11.806% by FSDT, 6.209% by HSDT, and 4.812 % by TSDT. Also, the applicability and accuracy of IHSDT for the evaluation of stresses is evident from the data obtained. The effect of radius of curvature to span ratio for 5, 10, 20, 50 and ∞ on the non-dimensional transverse deflection and stresses, a moderately thick shallow (a/h = 100) three layered symmetric [0/90/0] cross-ply square laminated composite shell is consider. The acquired and existing results are presented in Table 4.5.

Table 4.6: Non-dimensional central deflection of cross ply square with stacking sequence [0/90] and [0/90/90/0] under the effect UDL.

R/a	Theory	0°/90°		0°/90°/90°/0°	
		a/h=10	a/h=100	a/h=10	a/h=100
5	Present	17.3902	1.7521	10.6663	1.5333
	HSDT [a]	17.4886	1.7523	10.6356	1.5341
	HSDT [b]	17.5660	1.7519	10.4760	1.5332
	FSDT [b]	19.9440	1.7535	9.8249	1.5358
10	Present	18.5411	5.5388	11.1109	3.7203
	HSDT [a]	18.6543	5.5414	11.0775	3.7543
	HSDT [b]	18.7440	5.5388	10.9040	3.7208
	FSDT [b]	19.0650	5.5428	10.1410	3.7195
20	Present	18.8524	11.2674	11.2277	5.6679
	HSDT [a]	18.9699	11.2775	11.1936	5.6770
	HSDT [b]	19.0640	11.2680	11.0170	5.6660
	FSDT [b]	19.3650	11.2730	10.2220	5.6618
50	Present	18.9415	15.7092	11.2608	6.6259
	HSDT [a]	19.0601	15.7281	11.2265	6.6381
	HSDT [b]	19.1550	15.7110	11.0490	6.6234
	FSDT [b]	19.4520	15.7140	10.2450	6.6148
100	Present	18.9542	16.6399	11.2656	6.7892
	HSDT [a]	19.0731	16.6611	11.2312	6.8020
	HSDT [b]	19.1680	16.6420	11.0530	6.7866
	FSDT [b]	19.4640	16.6450	10.2490	6.7772
Plates	Present	18.9585	16.9748	11.2672	6.8455
	HSDT [a]	19.0774	16.9968	11.2328	6.8585
	HSDT [b]	19.1720	16.9800	11.0550	6.8427
	FSDT [b]	19.4690	16.9770	10.2510	6.8331

[a] Mantari et. al (2011); [b] Reddy et. al (1985)

Further, a simply supported two layered anti-symmetric [0/90] and four layered symmetric [0/90/90/0] cross-ply laminated composite square shell are considered for evaluate the bending behaviors in terms of non-dimensional transverse deflection. The influence of variation of radius of curvature to span ratio on the thick (a/h=10) and thin (a/h = 100) shell is also considered. In Table 4.6 obtained results and existing results due to TSDT by Mantari et al. (2011), HSDT and FSDT by Reddy et al. (1985) are presented. And also results for

plate as a special case is investigated and compared with various existing results. It is perceived from presented results that numerical values of non-dimensional deflection for thin shell is significantly lower than thick shell for both the laminated sequence. It is concluded from present results that as deflection in shell structure is directly proportional to radius of curvature value.

Further, to evaluate the bending response for cylindrical shell in terms of non-dimensional transverse deflection, a two layered anti-symmetric [0/90], three [0/90/0] and four [0/90/90/0] layered symmetric cross-ply laminated composite square cylinder is considered.

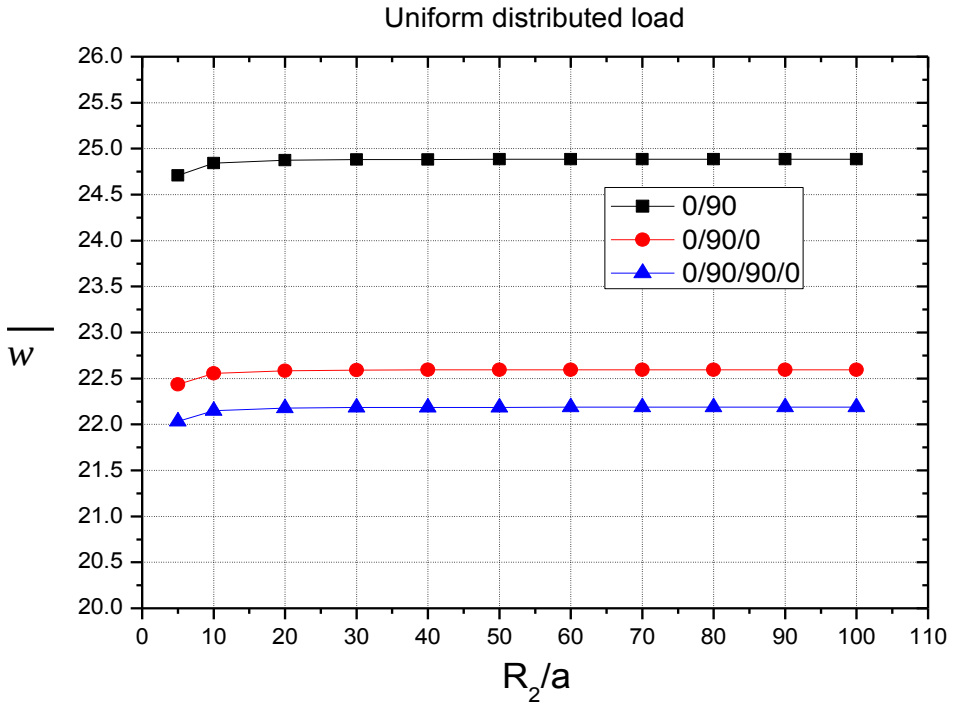

Figure 4.3: Transverse central deflection, with parametric variation of R_2/a, of a symmetric and anti-symmetric cross-ply laminated composite cylindrical shell under the effect of uniform load.

A variational study have been done for the non-dimensional deflection with respect to radius of curvature varied for 0 to 100 as shown in Fig 4.3. For this analysis span to thickness ratio is taken as a/h = 5 along with MP1 material properties. It is observed that the non-dimensional deflection show significant increment in value upto R/a = 20, onward there is not much variation in deflection value.

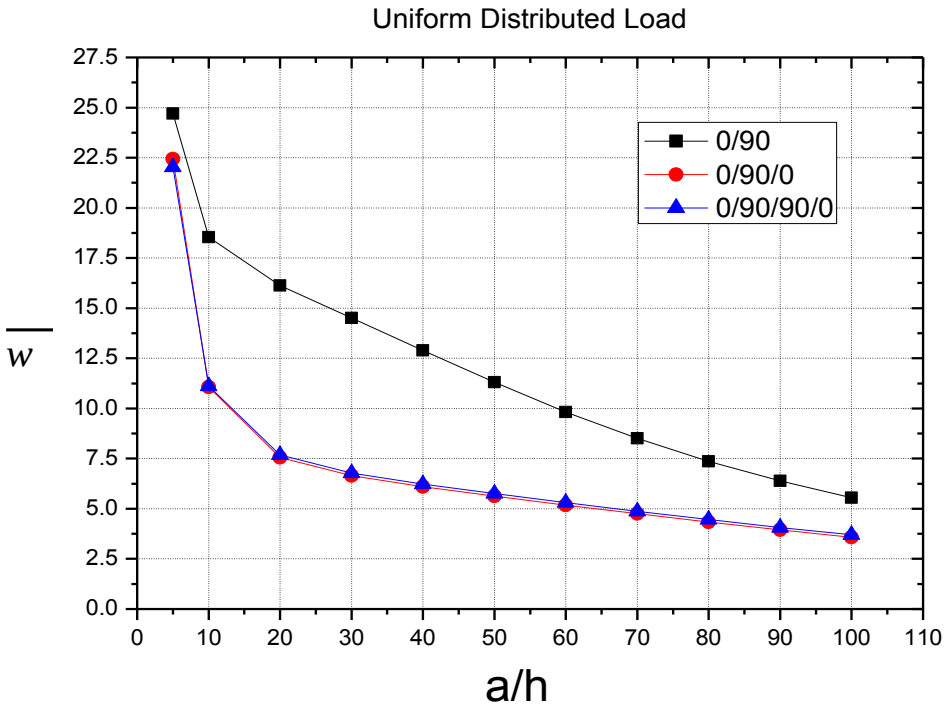

Figure 4.4: Transverse central deflection, with parametric variation of a/h, of a symmetric and anti-symmetric cross-ply laminated composite cylindrical shell under the effect of uniform load.

In Fig 4.4 show the variation of a/h on the non-dimensional transverse deflection at R/a = 5. It is observed that the trend of non-dimensional transverse deflection, with increase of a/h ratio for two, three and four layered cylindrical shells the decrease in deflection is noticed. Also noticed that trend of both symmetric laminated are almost same.

4.2.3. Multi-layered spherical and cylindrical shells under central point transverse load.

A simply supported two layered anti-symmetric, three and four layered symmetric cross-ply square spherical is consider to evaluate the bending behavior of non-dimensional transverse deflection for point load which is applied at the centre of the spherical shells. The results are presented for thick and thin spherical shells ($R_1 = R_2 = R$) for all three stacking sequence. The deflection is presented for radius to curvature to span thickness varies form 5, 10, 20, 50, 100 and also plate as a special case also considered using MP1 material properties. The obtained and existing results from HSDT by Mantari (2014), HSDT and FSDT by Reddy et. al (1854) presented in table 4.7. It is observed from obtained results for all three laminated sequences that the numerical value of deflection in thick shells is comparatively higher as in thin shell.

Table 4.7: Non-dimensional central deflection of cross ply square with stacking sequence [0/90], [0/90/0] and [0/90/90/0] under the effect point load for thin and thick spherical shell.

R/a	Theory	0°/90°		0°/90°/0°		0°/90°/90°/0°	
		a/h=10	a/h=100	a/h=10	a/h=100	a/h=10	a/h=100
5	Present	5.5896	0.8151	4.3081	0.6966	4.2336	0.6316
	HSDT [a]	5.7174	0.8212	4.3665	0.7029	4.3025	0.6383
	HSDT [b]	5.8953	-	4.4340	-	4.3574	-
	FSDT [b]	7.1015	-	5.1410	-	4.9360	-
10	Present	5.8780	1.8289	4.4269	1.3346	4.3493	1.2192
	HSDT [a]	6.0098	1.8358	4.4831	1.3418	4.4175	1.2268
	HSDT [b]	6.1913	-	4.5470	-	4.4690	-
	FSDT [b]	7.3836	-	5.2273	-	5.0186	-
20	Present	5.9560	3.2708	4.4580	1.8582	4.3796	1.7172
	HSDT [a]	6.0888	3.2796	4.5137	1.8666	4.4476	1.7261
	HSDT [b]	6.2714	-	4.5765	-	4.4982	-
	FSDT [b]	7.4692	-	5.2594	-	5.0496	-
50	Present	5.9782	4.3756	4.4669	2.1085	4.3882	1.9591
	HSDT [a]	6.1115	4.3866	4.5224	2.1176	4.4562	1.9688
	HSDT [b]	6.2943	-	4.5849	-	4.5065	-
	FSDT [b]	7.4909	-	5.2657	-	5.0557	-
100	Present	5.9814	4.6066	4.4681	2.1508	4.3894	2.0002
	HSDT [a]	6.1147	4.6182	4.5236	2.1601	4.4574	2.0100
	HSDT [b]	6.2976	-	4.5861	-	4.5077	-
	FSDT [b]	7.4940	-	5.2666	-	5.0565	-
Plate	Present	5.9814	4.6066	4.4685	2.1654	4.3899	2.0144
	HSDT [a]	6.1158	4.7014	4.5240	2.1747	4.4578	2.0242
	HSDT [b]	6.2987	-	4.5865	-	4.5081	-
	FSDT [b]	7.4853	-	5.2572	-	5.0472	-

[a] Mantari et. al (2011); [b] Reddy et. al (1985)

The effect of radius of curvature (R/a) keeping $R_1 \rightarrow \infty$ on the two, three and four layered stacking sequence of cross-ply laminated composite cylindrical shell. The span to thickness ratio is taken as a/h = 5 and MP1 material properties is considered. The radius of curvature varies from 5 to 100 and trend is plotted in Fig 4.5. It is noticed that initially deflection trend started from higher value and continuously decreasing as radius of curvature increase. Further, one more example is taken to show the trend of non-dimensional transverse deflection with respect to span to thickness ratio at R/a = 5. It is clearly observed form the Fig.4.6 that as span to thickness ratio increase the deflection in the laminated composite cylindrical shell decrease continually.it also concluded that sequence of plots of three and four layers are almost similar.

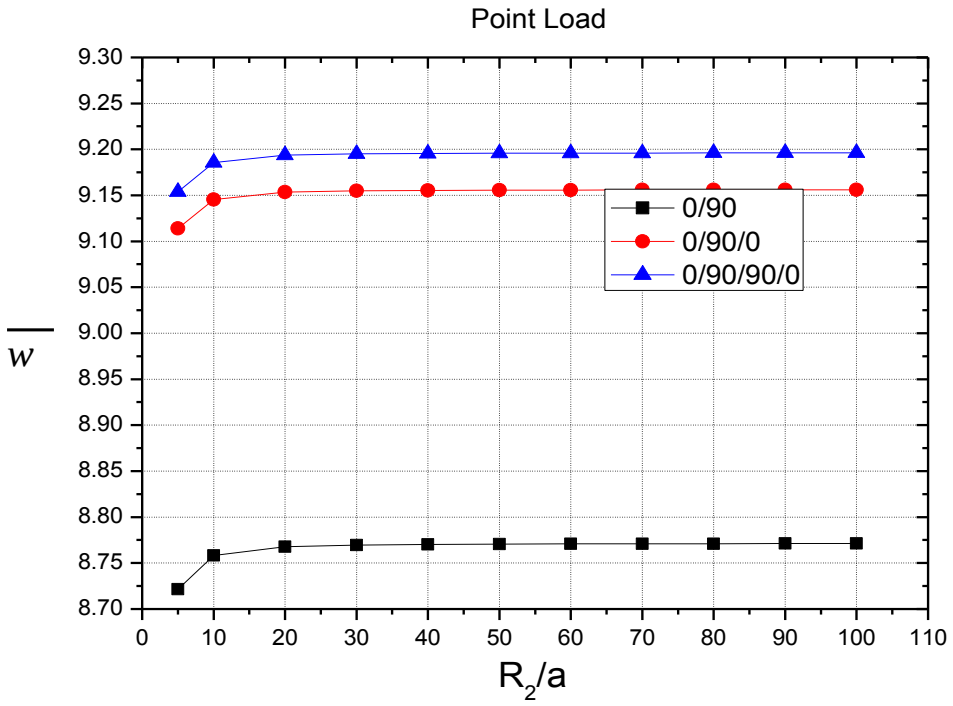

Figure 4.5: Transverse central deflection, with parametric variation of R_2/a, of a symmetric and anti-symmetric cross-ply laminated composite cylindrical shell under the effect of point load at the centre.

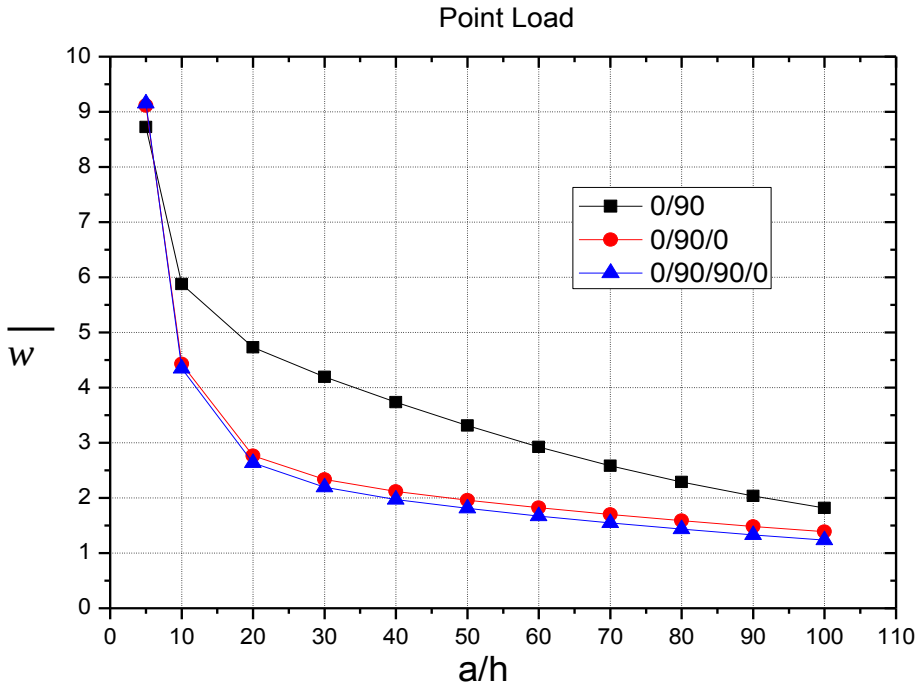

Figure 4.6: Transverse central deflection, with parametric variation of a/h, of a symmetric and anti-symmetric cross-ply laminated composite cylindrical shell under the effect of point load at the centre.

4.3. Static analysis of laminated composite shell using finite element method

In this session, a Finite element method approach is used to investigate the bending behaviour of laminated composite spherical and cylindrical shell for various boundary condition and validation of results is given by comparing with analytical solution for simply supported boundary condition. Using the developed finite element model a MATLAB code is developed for stiffness matrix and force matrix to get the response for non-dimensional transverse deflection for cross-ply laminated composite shell. The various boundary condition for confine the edges of square cross-ply laminated composite shell are shown below:

- Simple supported boundary condition (SS1)

  $u_\circ = w_\circ = \varphi_1 = \theta_1 = 0$ at x=0,a

  $v_\circ = w_\circ = \varphi_2 = \theta_2 = 0$ at y=0,b

- All edge clamped (CCCC)

  $u_\circ = v_\circ = w_\circ = \varphi_1 = \varphi_2 = \theta_1 = \phi_2 = 0$ at x=0,a and y=0,b

4.3.1. Finite element solution convergence

In order to investigate the convergence of finite element solution for non-dimensional transverse deflection, a symmetric 3-layered cross-ply square laminated composite shell is consider.

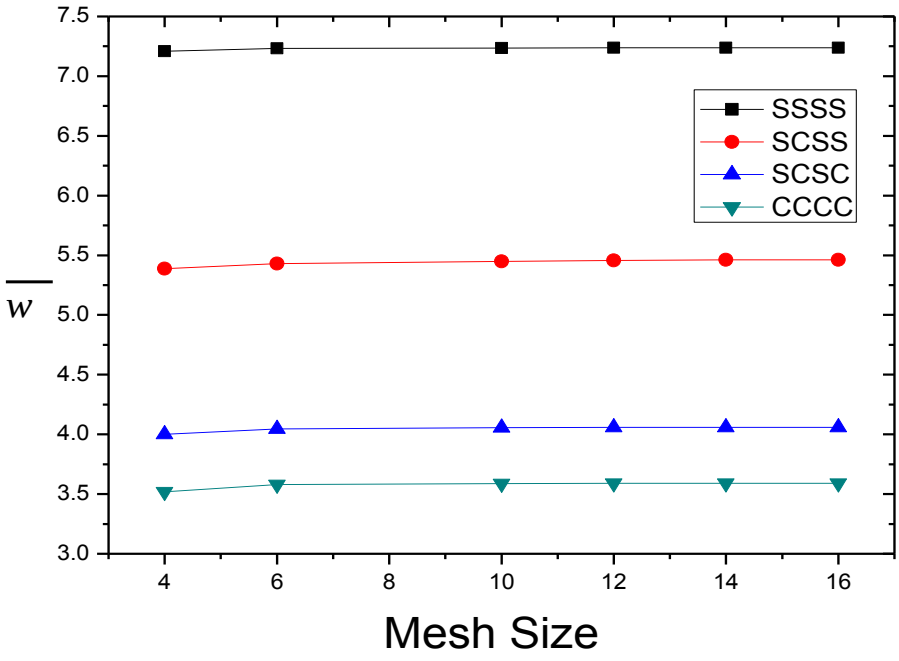

Figure 4.7: Convergence of finite element solution for symmetric 3-layred cross-ply laminated composite shell under effect of SSL.

The square spherical shell under the effect of sinusoidal load and subjected to SSSS, SCSS, SCSC and CCCC boundary conditions with MP1 material properties is considered. The span to thickness ratio (a/h) is taken as 10 along with radius to curvature to span (R/a) ratio is taken as 10. The mesh size varies from 4x4 to 16x16 and plotted in Fig. 4.7. The percentage difference between 12 and 14 mesh size is 0.001% .so it is clearly observed that numerical results convergences at 12 mesh size for the non-dimensional transverse deflection.

4.3.2. Multi-layered spherical and cylindrical shells under sinusoidal load.

A 2-layered [0/90] anti-symmetric and symmetric 3-layered [0/90/0] and 4-layered [0/90/90/0] square cross-ply laminated composite shell is considered to analysis the bending behaviour under the effect of sinusoidal loading condition.

Table 4.8: Numerical solution for non-dimensional deflection of anti-symmetric and symmetric cross-ply laminated composite shell under the effect of SSL.

R/a	Theory	0°/90°		0°/90°/0°		0°/90°/90°/0°	
		a/h=10	a/h=100	a/h=10	a/h=100	a/h=10	a/h=100
5	Present-FEM	11.1601	1.1929	6.9577	1.0316	6.9088	1.0259
	Present-IHSDT	11.0382	1.1937	6.9522	1.0323	6.9098	1.0265
	HSDT[a]	11.1660	1.1937	6.7688	1.0321	6.7865	1.0264
	FSDT [a]	11.1660	1.1948	6.4253	1.0337	6.3623	1.0279
10	Present-FEM	11.8889	3.5690	7.2368	2.4086	7.1860	2.4007
	Present-IHSDT	11.7504	3.5732	7.2307	2.4107	7.1869	2.4029
	HSDT [a]	11.8960	3.5733	7.0325	2.4099	7.0536	2.4024
	FSDT [a]	12.1230	3.5760	6.6247	2.4109	6.5595	2.403
20	Present-FEM	12.0863	7.1095	7.3101	3.6147	7.2588	3.6102
	Present-IHSDT	11.9431	7.1229	7.3038	3.6188	7.2597	3.6145
	HSDT [a]	12.0940	7.1236	7.1016	3.6170	7.1237	3.6133
	FSDT [a]	12.3090	7.1270	6.6756	3.6150	6.6099	3.6104
50	Present-FEM	12.1427	9.8437	7.3308	4.2042	7.2794	4.2031
	Present-IHSDT	11.9982	9.8679	7.3245	4.2095	7.2803	4.2087
	HSDT [a]	12.1500	9.8692	7.1212	4.2071	7.1436	4.2071
	FSDT [a]	12.3620	9.8717	6.6902	4.2027	6.6244	4.2015
Plate	Present-FEM	12.1535	10.6218	7.3348	4.3390	7.2833	4.3389
	Present-IHSDT	12.0087	10.6496	7.3285	4.3445	7.2843	4.3447
	HSDT [a]	12.1610	10.6510	7.1250	4.3420	7.1474	4.3430
	FSDT [a]	12.3730	10.6530	6.6939	4.3370	6.6280	4.3368

[a] Reddy et. al (1985)

The non-dimensional deflection for thick a/h = 10 and thin a/h = 100 are provided in table 4.8 with the variation of radius to span ratio taken as 5, 10, 20, 50, 100 and ∞. The mesh size 12x12 is considered to evaluate the non-dimensional transverse deflection. The validation of results presented by FEM formulation is compared with analytical solution presented by presented IHSDT, HSDT and FSDT by Reddy et al. (1985).

It is observed from the results that the present finite element results have a close agreement with the closed form solution of present IHSDT for non-dimensional deflection for the spherical shell as well as for the plate.

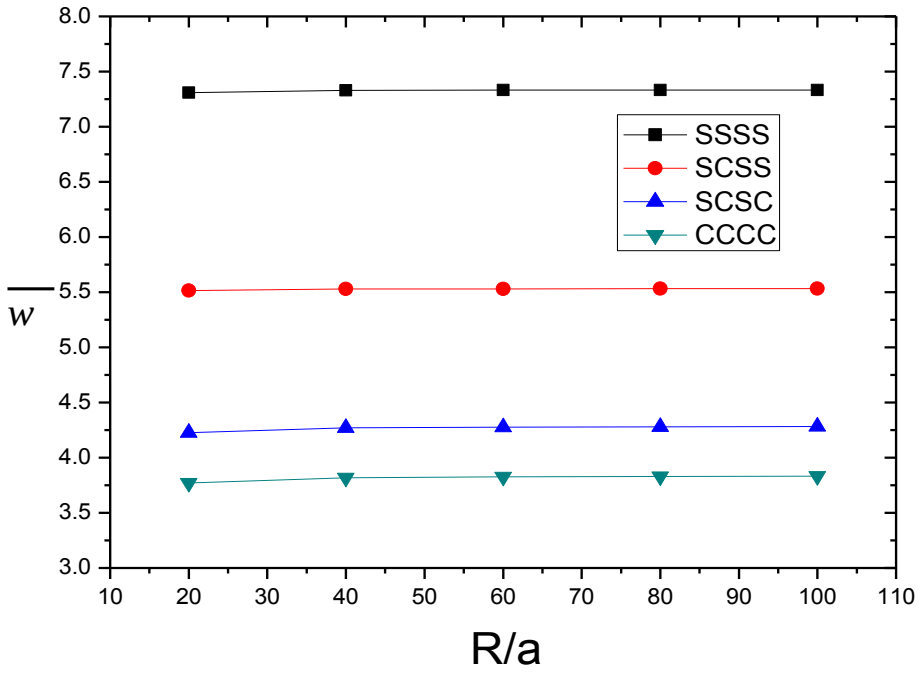

Figure 4.8: Effect of different boundary conditions on the non-dimensional transverse deflection for thick cross-ply laminated spherical shell under the effect of SSL.

Further, a three layered [0/90/0] symmetric cross-ply laminated composite spherical shell is considered having material properties MP1. The shell is subjected to sinusoidal transverse load. The effect of variation of radius of curvature to span ratio (*R/a*) for thick (*a/h*=10) and thin (*a/h*=100) spherical shell on non-dimensional transverse deflection is presented in Figs. (4.8-4.9) for various boundary conditions. For both the cases, the non-dimensional deflection increases with increase in radius to span ratio. However, the rate of increment in non-dimensional deflection is higher in case of the thin shell as compared to thick shell irrespective of the boundary conditions.

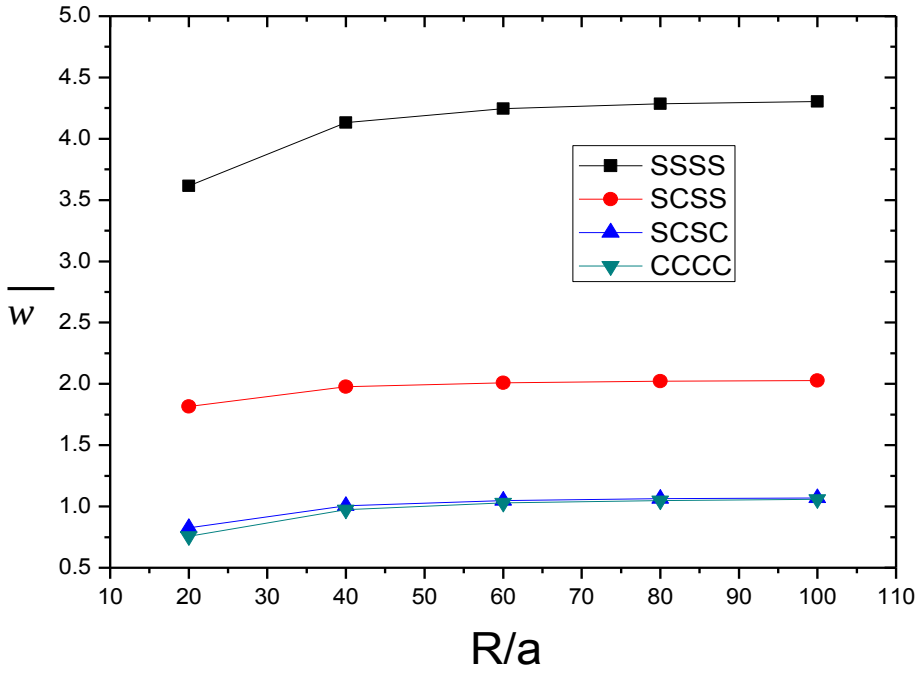

Figure 4.9: Effect of different boundary conditions on the non-dimensional transverse deflection for thin (a/h=100) cross-ply laminated spherical shell.

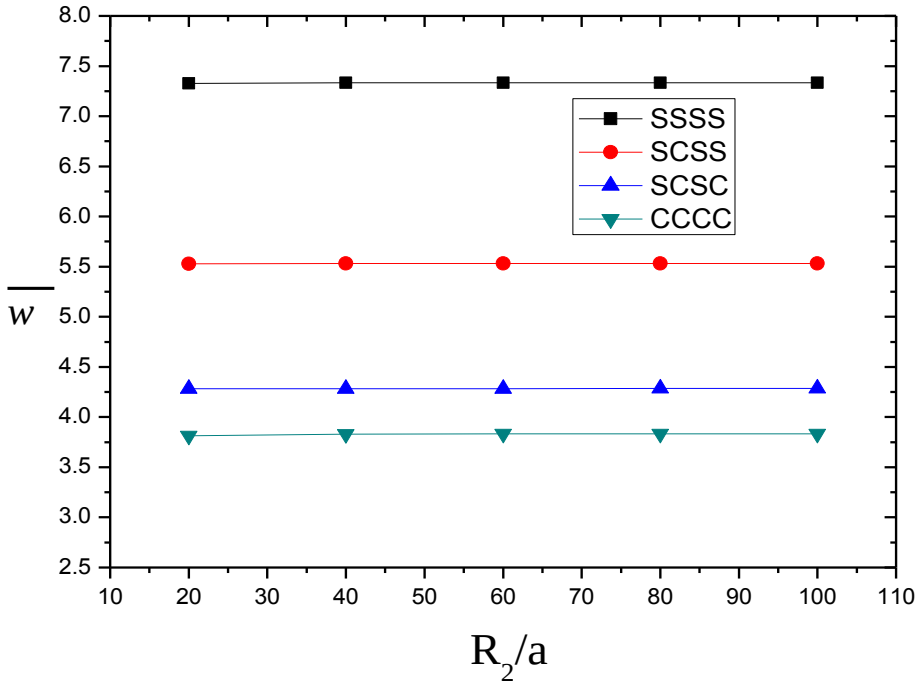

Figure 4.10: Effect of different boundary conditions on the non-dimensional transverse deflection for thick (a/h=10) cross-ply laminated cylindrical shell under the effect of SSL.

Further, to study the effect of different boundary condition on non-dimensional deflection for cross-ply laminated composite cylinder ($R_1 = \infty$ and $R_2 = R$) under SSL condition. A 3-layered [0/90/0] symmetric square (a = b) l=cross-ply laminated composite cylindrical shell is considered. The non- dimensional deflection is evaluated for thick (a/h=10) in Fig. 4.10, also results for thin (a/h=100) is shown in Fig. 4.11 using MP1 material properties.

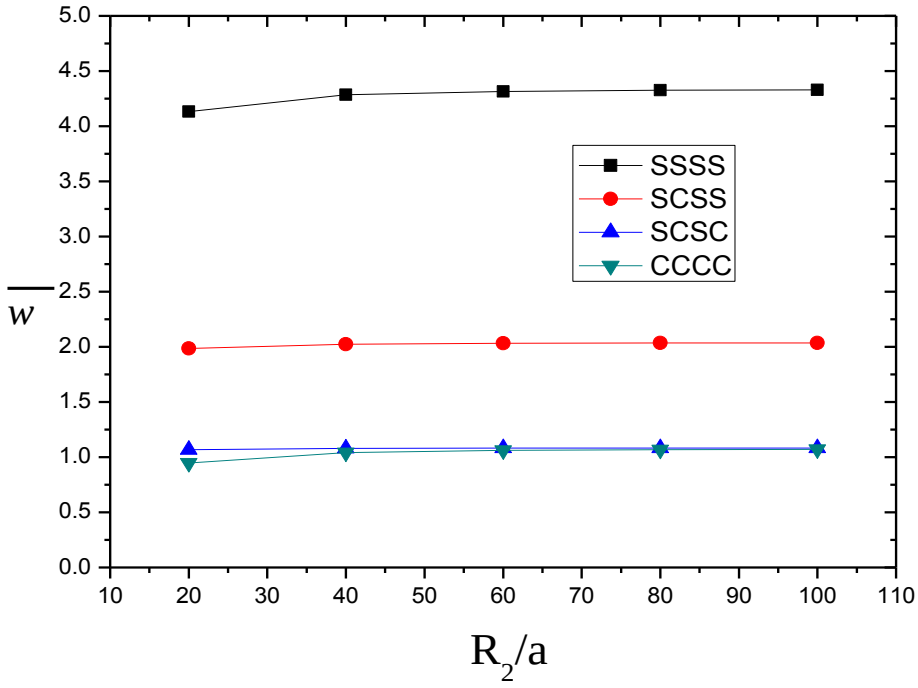

Figure 4.11: Effect of different boundary conditions on the non-dimensional transverse deflection for thin (a/h=100) cross-ply laminated cylindrical shell under the effect of SSL.

It is observed for Fig 4.10 that different boundary condition shown not much significant variation in non-dimensional transverse deflection. The rate of change of deflection shows marginal change for various radius to span ratio. Also for Fig 4.11, the effect of SCSC and CCCC on thin cylindrical shell is almost same throughout. More over in SSSS boundary condition, initially non-dimensional deflection increase.

4.3.2. Multi-layered spherical and cylindrical shells under uniform distributed load.

A bending behaviour of anti-symmetric and symmetric cross-ply square laminated composite spherical shell is considered to show the comparison between FEM numerical solution, IHSDT analytical solution along with Reddy's HSDT and FSDT. For this problem

Table 4.9: Numerical solution for non-dimensional deflection of anti-symmetric and symmetric cross-ply laminated composite shell under the effect of UDL.

R/a	Theory	0°/90°		0°/90°/0°		0°/90°/90°/0°	
		a/h=10	a/h=100	a/h=10	a/h=100	a/h=10	a/h=100
5	Present-FEM	17.5569	1.7536	10.6350	1.5100	10.6670	6.8418
	Present-IHSDT	17.3902	1.7521	10.6241	1.5094	10.6663	1.5333
	HSDT [a]	17.5660	1.7519	10.3320	1.5092	10.4760	1.5332
	FSDT [a]	19.9440	1.7535	9.7937	1.5118	9.8249	1.5358
10	Present-FEM	18.7346	5.5386	11.0796	3.6456	11.1117	3.7205
	Present-IHSDT	18.5411	5.5388	11.0677	3.6439	11.1109	3.7203
	HSDT[a]	18.7440	5.5388	10.7520	3.6426	10.9040	3.7208
	FSDT [a]	19.0650	5.5428	10.1100	3.6445	10.1410	3.7195
20	Present-FEM	19.0535	11.2552	11.1965	5.5544	11.2286	5.6661
	Present-IHSDT	18.8524	11.2674	11.1843	5.5531	11.2277	5.6679
	HSDT[a]	19.0640	11.2680	10.8620	5.5503	11.0170	5.6660
	FSDT [a]	19.3650	11.2730	10.1910	5.5459	10.2220	5.6618
50	Present-FEM	19.1447	15.6816	11.2296	6.4938	11.2617	6.6227
	Present-IHSDT	18.9415	15.7092	11.2173	6.4933	11.2608	6.6259
	HSDT [a]	19.1550	15.7110	10.8930	6.4895	11.0490	6.6234
	FSDT [a]	19.4520	15.7140	10.2140	6.4827	10.2450	6.6148
Plate	Present-FEM	19.1622	16.942	11.2359	6.7091	11.2681	6.8418
	Present-IHSDT	18.9585	16.9748	11.2237	6.7087	11.2672	6.8455
	HSDT [a]	19.1720	16.9800	10.2200	6.7047	11.0550	6.8427
	FSDT [a]	19.4690	16.9770	10.8990	6.6970	10.2510	6.8331

[a] Reddy et. al (1985)

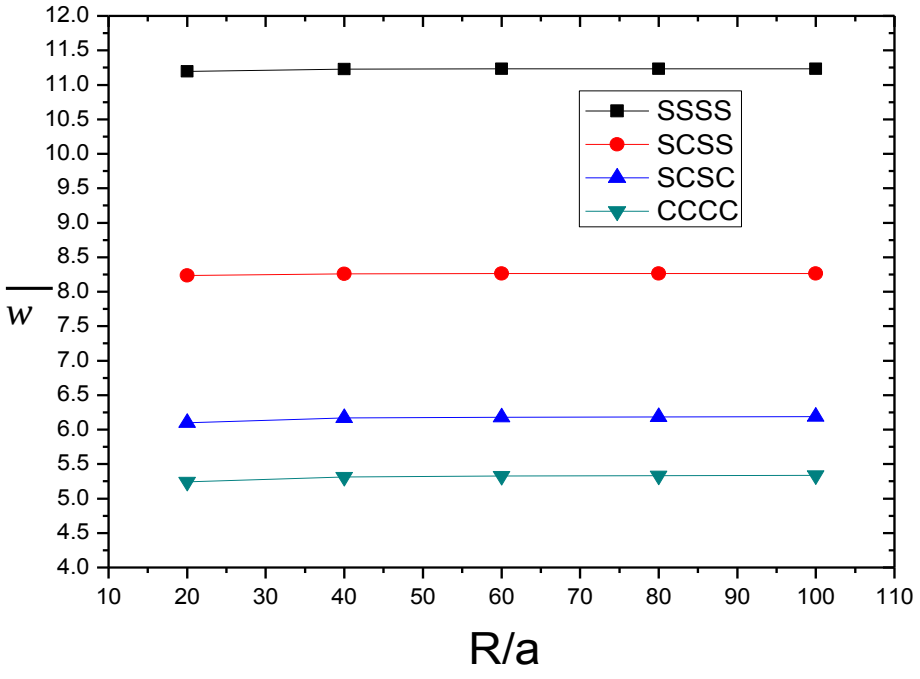

Figure 4.12: Effect of different boundary conditions on the non-dimensional transverse deflection for thick (a/h=10) cross-ply laminated spherical shell under the effect of UDL.

thick and thin shells are considered along with MP1 material properties. The results are obtained by using 12x12 mesh size also variation of radius to span ratio is shown in table 4.9. It is observed from the Numerical results present using finite element have a small variation with the closed form solution of present IHSDT for non-dimensional deflection for the Further, a three layered [0/90/0] symmetric cross-ply spherical shell is considered having material properties MP1. The shell is subjected to uniformly distributed load transverse load.

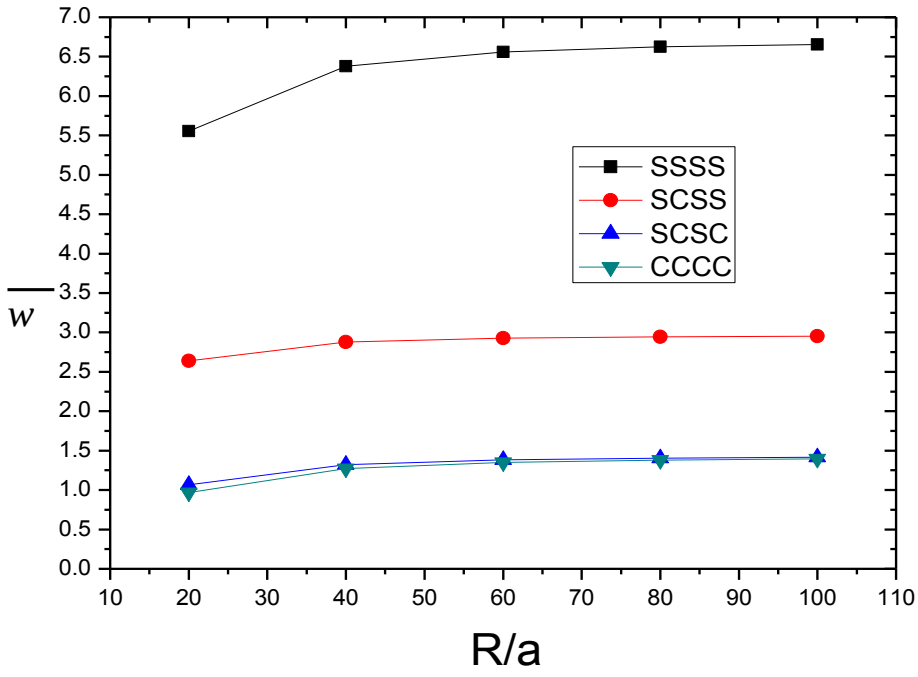

Figure 4.13: Effect of different boundary conditions on the non-dimensional transverse deflection for thin (a/h=100) cross-ply laminated spherical shell under the effect of UDL

The effect of radius to span ratio for thick (a/h=10) and thin (a/h=100) shell on non-dimensional deflection is presented in Figs. (4.12-4.13) for various boundary conditions. For both the cases, the non-dimensional deflection increases with increase in radius to span ratio. However, the rate of increment in non-dimensional deflection is higher in case of the thin shell as compared to thick shell irrespective of the boundary conditions.

For both the cases, the non-dimensional deflection increases with increase in radius to span ratio. However, the rate of increment in non-dimensional deflection is higher in case of the thin shell as compared to thick shell irrespective of the boundary conditions.

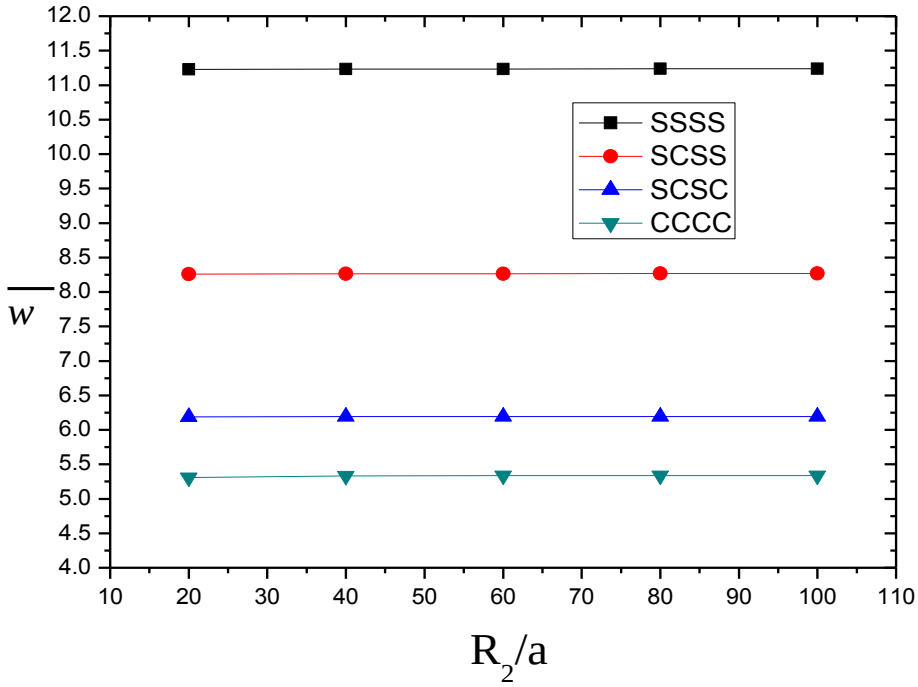

Figure 4.14: Effect of different boundary conditions on the non-dimensional transverse deflection for thick (a/h=10) cross-ply laminated cylindrical shell under the effect of UDL.

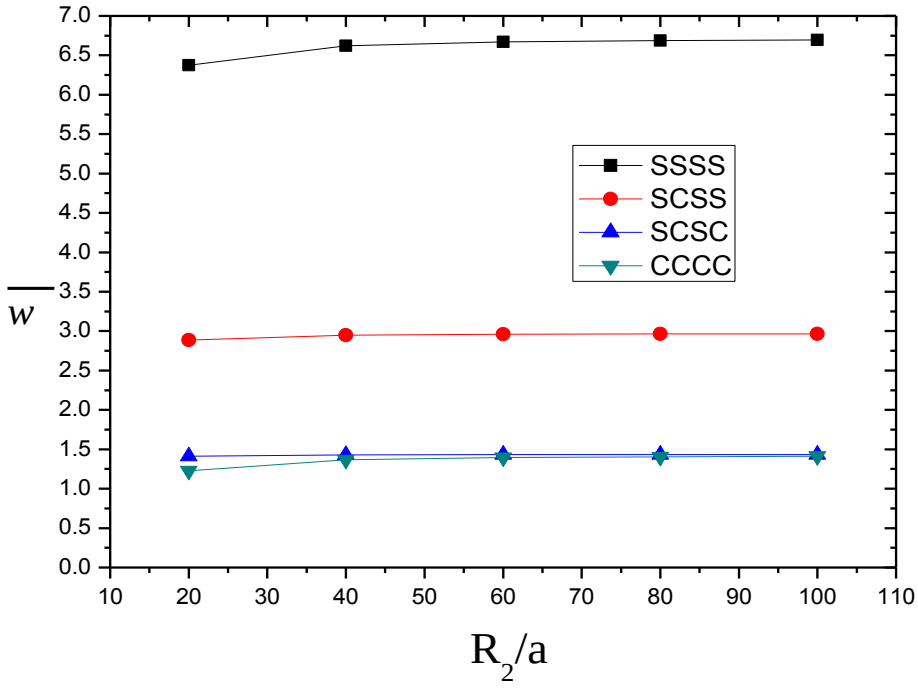

Figure 4.15: Effect of different boundary conditions on the non-dimensional transverse deflection for thin (a/h=100) cross-ply laminated cylinder shell under the effect of UDL.

Further, to study the effect of different boundary condition on non-dimensional deflection for cross-ply laminated composite cylinder ($R_1 = \infty$ and $R_2 = R$) under UDL condition. A 3-layered [0/90/0] symmetric square (a = b) cross-ply laminated composite cylindrical shell is considered. The non- dimensional deflection is evaluated for thick (a/h=10) in Fig. 4.14, also results for thin (a/h=100) is shown in Fig. 4.15 using MP1 material properties. It is observed from Fig 4.14, rate of increase of non- dimensional transverse deflection shows marginal change for different boundary conditions.

Fig 4.15, the non-dimensional deflection increases with increase in radius to span ratio for SSSS boundary condition. However, the rate of increment in non-dimensional deflection is higher in case of the thin shell as compared to thick shell irrespective of the boundary conditions.

4.4. Summary

The bending behaviour of cross-ply laminated composite spherical and cylindrical shell under the effect SSL, UDL and point load is considered and validated for various examples. The effect of span to thickness ratio and radius to span ratio on non-dimensional transverse deflection is shown for spherical and cylindrical shells. Moreover, the finite element solutions for the shells with various boundary conditions subjected to SSL and UDL are obtained. The analytical and finite element solutions based on IHSDT are obtained and compared with the established results in the literature.

Chapter 5 Conclusions and Scope of Future work

5.1. Conclusion

In the present work, IHSDT originally developed for plates is extended for the analysis of shell structures. The Navier- type closed form solution are developed for simply supported shells. Further, in order to enhance the applicability to general boundary and loading conditions, the numerical solutions in the framework of finite element analysis are also obtained. An eight noded isoparametric element is used to discretise the shell structure.

1. The bending behaviour for cross-ply laminated composite spherical and cylindrical shell are examined by presenting the close-form and finite element solution. The implemented of IHSDT for various loading condition give very close results to most accurate solution present in literature.
2. The increase in Radius of curvature to span ratio also shows the increase in non-dimensional transverse deflection for both SSL and UDL loading condition.
3. The percentage difference in case of SSL loading is 2.26% and 3.56% in case of UDL from the most accurate layer wise theories.
4. The effect of various boundary conditions on laminated composite cylindrical shells are observed.

On the basis of the present work, the following research articles are prepared:

- Lalit K. Sharma, Y. S. Joshan, Neeraj Grover. Transverse deformation and stress behavior of laminated composite spherical and cylindrical shells. Indian national conference of Applied Mechanics, 5 to 7- July 2017 at MNNIT, Allahabad. pp 23-24.
- Lalit K. Sharma, Neeraj Grover. The effects of micromechanical parameters on the bending behaviour of glass-epoxy laminated composite shells. (Accepted for International conference on Theoretical, Applied, Computational and Experimental mechanics- Dec 2017 at IIT, Kharagpur)
- Deformation and stresses behaviour of doubly curved laminated spherical and cylindrical shells under various transverse loads. (In preparation)

5.2. Scope of Future Work

1. The influence of micro-mechanical model on static analysis of laminated composite shell.
2. Static analysis of Functionally Graded shell structure using IHSDT.
3. Static and Finite element analysis of angle-ply laminated composite shell structures.

References

A. E. H. Love, “The Small Free Vibrations and Deformation of a Thin Elastic Shell.” Proceedings of the Royal Society of London, pp. 491-546, 1888.

Bhimaraddi, A. and L. K. Stevens. 1986. "On the Higher Order Theories in Plates and Shells," Int. J. Solids and Struct. , 6:35-50.

Bhimaraddi, “Three-dimensional elasticity solution for static response of orthotropic doubly curved shallow shells on rectangular planform,” composite structure, vol. 24, pp. 67-77, 1993.

Chandrashekar and Gopalakrishna P., “Transversely isotropic infinite cylindrical shell subjected to a radial axisymmetric line load.,” Fibre science and technology, vol 16, pp. 275-293, 1982.

Dong, S. B. and F. K. W. Tso. 1972. "On a Laminated Orthotropic Shell Theory Including Transverse Shear Deformation," ASME J. Appl. Mech ., 39:1091-1097.

Giunta G., Biscani F., Belouettar S. and Carrera E., “Hierarchical modelling of doubly curved laminated composite shells under distributed and localised loadings,” Composite: Part B, vol. 42, pp. 682-691, 2011.

Grover N., Maiti D. K. and Singh B. N., “A new inverse hyperbolic shear deformation theory for static and buckling analysis of laminated composite and sandwich plates,” Composite structure, vol. 95, pp. 667-675, 2012.

Hildebrand, F. B., E. Reissner and G. B. Thomas. 1949. "Notes on the Foundations of Small Displacements of Orthotropic Shells," NACA: TN-1833.

Kant, T. and C. K. Ramesh. 1976. ’Analysis of Thick Orthotropic Shells," Proc., I.A.S.S. World Congress on Space Enclosures, Montreal, Canada, pp. 401-409.

Khara R. K., T. Kant and A. K. Garg, “Closed-form thermo-mechanical solutions of higher -order theories of cross-ply laminated shallow shells,” composite structures, vol. 59, pp. 313-340, 2003.

Kant, T. 1981. "A Higher-Order General Laminated Shell Theory," Res. Rep. C/R/395/81, Civil Engg. Dept., Swansea, Univ. of Wales.

Mirsky, “Vibration of Orthotropic, thick, cylindrical shells,” The journal of the acoustical society of america, vol. 36, no. 1, pp. 42-51, 1964.

Murty, A. V. K. and T. S. R. Reddy. 1986. "A Higher Order Theory for Laminated Composite Cylindrical Shells," J. Aero. Society of India, pp. 161-171.

Naghdi, P. M. 1957. "On the Theory of Thin Elastic Shells," Quart. Appl. Math. , 14:369-380.

Noor AK, Burton WS. Assessment of computational models for multilayered composite shells. Appl Mech Rev 1990, 43: 67–97.

Oktem S. and Chaudhuri A. R, “Levy type Fourier analysis of thick cross-ply doubly curved panels”, Composite structure, vol. vol. 80, pp. 445-488, 2007.

Pagano N. J., “Exact solutions for rectangular bidirectional composite and sandwich plates.,” journal of composite materials, vol. 4, 1970.

Reddy J. N. and ASCE M., “Exact solution of moderately thick laminated shells,” journal of engineering mechanics, vol. vol. 110, no. 5, pp. 794-809, 1984.

Reddy J. N. and C. F. Liu, “A higher-order shear deformation theory of laminated elastic shells.,” Int. J Engng Sci, vol. vol 23, no. 3, pp. 319-330, 1985.

Reddy J., Mechanics of laminated composite plates and shells, 2nd ed., Florida: CRC Press , 2004.

Reissner, E. 1950. "On a Variational Theorem in Elasticity," J. Math. and Physics, 29:90-95

Ren G., “Analysis of simply-supported laminated circular cylindrical shell roofs,” composite structure, vol. 11, pp. 277-292, 1989.

Sanders J. L. Jr., “An improved first-approximation theory for thin shells.,” NASA TR-R24, 1959.

Tornabene Francesco, Fantuzzi Nicholas, Bacciocchi Michele, “On the mechanics of laminated doubly-curved shells subjected to point and line loads”, Int J. Engg Sci,109:115-164,2016

Liu BoA, Ferreira J.M, Xing Y.F., Neves A.M.A., “Analysis of functionally graded sandwich and laminated shells using a layerwise theory and a differential quadrature finite element method” , composite structure,136:546-553,2016.

Widera, G. E. O. and D. L. Logan. 1980. "Refined Theories for Non-Homogeneous Anisotropic Cylindrical Shells," ASCE J. of Engg. Mech. , 106:1053-1090.

Whitney, J. M. and C. T. Sun. 1974. "A Refined Theory for Laminated Anisotropic Cylindrical Shells," ASME J. Appl. Mech., 41:471-476.

Wu C. P., Tarn J. Q. and Chi S. M., Three-dimensional analysis of doubly curved laminated shells, *J. Eng. Mech.*, 122 (5) (1996) 391-401.